Sister Rod Destructive Examinations (FY20)

Appendix E: Mechanical Testing

Spent Fuel and Waste Disposition

Prepared for
US Department of Energy

Spent Fuel and Waste Science and Technology

Oak Ridge National Laboratory
Rose Montgomery,
Yong Yan, Ben Garrison

November 30, 2020

M2SF-21OR010201032

ORNL/SPR-2020/1790

SUMMARY

This report documents work performed under the Spent Fuel and Waste Disposition's Spent Fuel and Waste Science and Technology program for the US Department of Energy (DOE) Office of Nuclear Energy (NE). This work was performed to fulfill Level 2 Milestone M2SF-21OR010201032, "ORNL High Burnup Confirmatory Demo Sibling Rod Testing Results," within work package SF-21OR01020103 and is an update to the work reported in M2SF-19ORO010201026 and M2SF-19OR010201028.

As a part of the DOE NE High Burnup Spent Fuel Data Project, Oak Ridge National Laboratory (ORNL) is performing destructive examinations (DEs) of high burnup (HBU) (>45 GWd/MTU) spent nuclear fuel (SNF) rods from the North Anna Nuclear Power Station operated by Dominion Energy. The SNF rods, called *sister rods* or *sibling rods*, are all HBU and include four different kinds of fuel rod cladding: standard Zircaloy-4 (Zirc-4), low-tin Zirc-4, ZIRLO, and M5. The DEs are being conducted to obtain a baseline of the HBU rod's condition before dry storage and are focused on understanding overall SNF rod strength and durability. Composite fuel and defueled cladding will be tested to derive material properties. Although the data generated can be used for multiple purposes, one primary goal for obtaining the post-irradiation examination data and the associated measured mechanical properties is to support SNF dry storage licensing and relicensing activities by (1) addressing identified knowledge gaps and (2) enhancing the technical basis for post-storage transportation, handling, and subsequent disposition.

This report documents the status of the ORNL Phase 1 DE activities related to the mechanical testing of selected sister rods in Phase 1 of the sister rod test program.

Table ES-1 summarizes the mechanical test status.

Table ES-1. DE status.

Planned DE		Status	Comments
DE.07	Conduct four-point bend (4PB) tests	In progress	All Phase 1 tests, except for those planned for aerosol collection, are complete. Tests were conducted at both room temperature (RT) and at 200°C. Data evaluation is in progress. The flexural strength and strain at fracture, 0.2% offset yield strength, and flexural modulus were calculated for the tests completed. Generally, the heat-treated M5 and ZIRLO-clad specimens have higher ductility than the baseline specimens, but it is difficult to come to any firm conclusions about whether the heat treatments affected specimen performance with the limited data available. Additional evaluations of the data will be completed in FY21. The mass loss from the specimen resulting from fracture was measured during the 4PB tests. There was not a trend of pellet mass loss related to test temperature, although the RT fractures seemed more energetic than the 200°C fracture. With each pellet weighing approximately 5.1–7.0 g, the maximum mass released from the cladding represents about one-quarter of a pellet, whereas the more typical 0.4 g mass released is less than one-tenth of a full pellet

Planned DE		Status	Comments
DE.08	Conduct axial tensile tests	In progress	Specimen preparation in progress.
DE.09	Test for American Society for Testing and Materials (ASTM) microhardness	Not started	Equipment is available.
DE.10	Conduct fueled ring compression tests (RCT)	Complete	Complete. There is no appreciable difference in the maximum load-bearing capability of the segments from RT to 200°C. Cladding type also does not greatly influence the load-bearing capability, and there does not appear to be a difference related to the heat-treatment applied to some of the rods. The main observed variant is the orientation of the major cracks in the pellet because these appear to nucleate fracture of the adjacent cladding and determine the pellet fracture plane. The observed transverse bearing load of the specimen is 16.4 kN (3,690 lb_f) on average with a minimum load-bearing capability of 12.3 kN (2,766 lb_f) for the tested segments.
DE.14	Perform burst tests	Not started	Equipment must be evaluated and modified for testing at the proposed pressure and temperature.

ACKNOWLEDGMENTS

Many thanks to our US Department of Energy Office of Nuclear Energy sponsor, Ned Larson, along with the Spent Fuel and Waste Science and Technology storage and transportation program leadership for their continued support. The sister rod project would not have been possible without the vision and support of the Electric Power Research Institute, Westinghouse, Framatome, and Dominion Energy.

This work would not have been possible without the support and expertise provided by the leadership and staff members of the ORNL's Irradiated Fuel Examination Laboratory. Special thanks go to Jerid Metcalf, Scott Thurman, John Hinds, and Brian Woody for their assistance with in-cell testing activities. We also appreciate Bob Morris' assistance in cutting the test specimens. Rick Henry has the unenviable task of tracking the bits and pieces of sister rods and their moves around the hot cell and to other facilities, and we very much appreciate his patience and continued support. Jim Miller, Mark Delph, and Russ Smith have been vital in supporting the deployment of new equipment to the cell, and we appreciate their continued support.

This page is intentionally left blank.

CONTENTS

SUMMARY ..... E-iii
ACKNOWLEDGMENTS ..... E-v
CONTENTS ..... E-vii
LIST OF FIGURES ..... E-ix
LIST OF TABLES ..... E-xi
REVISION HISTORY ..... E-xiii
ACRONYMS ..... E-xv
E-1. Mechanical Test Frame Installation E-1
E-2. Four-Point Bend Tests E-3
E-2.1 Test Procedure and Data Processing E-5
E-2.1.1 Test Protocol E-5
E-2.1.2 Test Specimen E-5
E-2.1.3 Data Reduction E-5
E-2.2 Load and Displacement Data E-8
E-2.3 Corrections for Machine Compliance E-8
E-2.4 Calculated Stress, Strain, 0.2% Offset Yield, Flexural Strength, and Flexural Rigidity E-8
E-2.5 Typical Fracture Observed E-19
E-2.6 Fuel Release During Fracture E-21
E-3. Axial Tension Testing E-24
E-4. Microhardness Tests E-25
E-5. Ring Compression Tests E-25
E-5.1 Test Procedure and Data Processing E-25
E-5.1.1 Test Protocol E-25
E-5.1.2 Test Specimen E-26
E-5.1.3 Data Reduction E-26
E-5.2 Peak Load Data E-28
E-5.3 Typical Fracture Observed E-31
E-6. Burst Tests E-32
References E-32

This page is intentionally left blank.

LIST OF FIGURES

Figure E-1. The Instron load frame with its furnace was moved to the hot cell loading bay (left) and into the hot cell through the cell's primary airlock (right). E-2
Figure E-2. The Instron load frame, with its furnace, was placed in the north hot cell (left) followed by the installation of the service plug containing all instrumentation and power (right). E-2
Figure E-3. The load frame configured for 4PB tests of a sister rod specimen. E-3
Figure E-4. Simple beam representation of the 4PB test. E-6
Figure E-5. Zirc-4 and LT Zirc-4 specimens, load vs. crosshead extension. E-10
Figure E-6. M5 specimens, load vs. crosshead extension. E-11
Figure E-7. ZIRLO specimens, load vs. crosshead extension. E-12
Figure E-8. Load vs. crosshead extension for all RT tests. E-13
Figure E-9. Load vs. crosshead extension for all 200°C tests. E-14
Figure E-10. Stress vs. strain plot for RT data. E-15
Figure E-11. Stress vs. strain plot for 200°C data. E-16
Figure E-12. Calculated RT data plotted as a function of specimen average burnup. E-17
Figure E-13. Calculated 200°C data plotted as a function of specimen average burnup. E-18
Figure E-14. (a) Many specimens did not completely fracture and (b) fractured at pellet-pellet interfaces. E-19
Figure E-15. (a) An example of through-section fracture with secondary tearing, and (b) fracture that occurred in the body of the pellet. E-20
Figure E-16. Histogram of mass loss resulting in 4PB test. E-21
Figure E-17. Measured specimen mass differential (pretest and posttest) as a function of estimated average specimen burnup. E-22
Figure E-18. (a) Posttest debris was captured by a catch tray located below the specimen with (b) the typical RT debris field composed of small particles. E-23
Figure E-19. Typical test specimen. E-26
Figure E-20. Typical load vs. crosshead displacement for fueled RCT. E-27
Figure E-21. Measured Load Frame Compliance Used to Correct RCT data. E-27
Figure E-22. Maximum RCT load vs. estimated average specimen burnup at RT and 200°C RCT. E-29
Figure E-23. Maximum RCT load vs. average specimen burnup at RT for baseline and FHT specimens. E-29
Figure E-24. Comparison of Load vs. Crosshead Displacement for a ZIRLO Sister Rod Specimen, Fueled and Defueled. E-30
Figure E-25. Typical post-RCT appearance. E-31
Figure E-26. RCT fracture path along major pellet crack. E-32

This page is intentionally left blank.

LIST OF TABLES

Table ES-1. DE status. ..... E-iii

Table E-1. List of specimens for 4PB. E-4
Table E-2. Measured and calculated 4PB data. E-9
Table E-3. List of specimens for axial tension testing. E-24
Table E-4. RCT peak load data. E-28

This page is intentionally left blank.

REVISION HISTORY

Date	Changes
10/29/2020	This appendix contains new information on the mechanical testing results.
11/30/2020	Comments received on the 10/29/2020 draft were incorporated and the document numbering revised to reflect its M2 status.

This page is intentionally left blank.

ACRONYMS

4PB	four-point bend
ANL	Argonne National Laboratory
ASTM	American Society for Testing and Materials
DE	destructive examination
DOE	US Department of Energy
FHT	full-length fuel rod heat treatment
HBU	high burnup
LT	low tin
NE	Office of Nuclear Energy
ORNL	Oak Ridge National Laboratory
RCT	ring compression tests
RT	room temperature
SNF	spent nuclear fuel

This page is intentionally left blank.

E-1. Mechanical Test Frame Installation

As a part of the DOE NE High Burnup Spent Fuel Data Project [E-1], Oak Ridge National Laboratory (ORNL) is performing destructive examinations (DEs) of high burnup (HBU) (>45 GWd/MTU) spent nuclear fuel (SNF) rods from the North Anna Nuclear Power Station operated by Dominion Energy. The SNF rods, called *sister rods* or *sibling rods*, are all HBU and include four different kinds of fuel rod cladding: standard Zircaloy-4 (Zirc-4), low-tin (LT) Zirc-4, ZIRLO, and M5. The Phase 1 DEs [E-2, E-3] are being conducted to obtain a baseline of the HBU rod's condition before dry storage and are focused on understanding overall SNF rod strength and durability. Composite fuel and defueled cladding will be tested to derive material properties. Although the data generated can be used for multiple purposes, one primary goal for obtaining the postirradiation examination data and the associated measured mechanical properties is to support SNF dry storage licensing and relicensing activities by (1) addressing identified knowledge gaps and (2) enhancing the technical basis for post-storage transportation, handling, and subsequent disposition.

To provide the capability for mechanical testing, a large Instron load frame (65 × 31 × 29 in.) with a 30 kN capacity (~1 ton of loading force) was installed in the Irradiated Fuels Examination Facility north hot cell. The cell location was selected based on its accessibility and its lower dose rates (~150 R/h).

During FY20, the load frame was modified for durability in the radiation field and to provide remote manipulation capabilities. Lead shielding was placed around the load frame's instrumentation string to provide more protection from radiation damage.

The load frame was successfully installed in the cell in June 2020. It was carefully rigged, lifted, and transported to the hot cell loading bay (Figure E-1, left) where it was placed on a forklift. The rigging was left in place for in-cell handling. The load frame was moved to the hot cell charging area and then moved into the cell using the primary airlock ((Figure E-1, right). From there, the in-cell crane used the same rigging to lift the load frame and move it to the north cell operating position, as shown in Figure E-2 (left). Standard bubble levels were used to check the level and plumb of the installed load frame.

To connect the control unit in the operating area of the hot cell with the load frame in the cell, instrumentation and power cabling were run through the cell's 3 ft thick wall using a service plug. As shown in Figure E-2 (right), this requires removing the existing plug, which momentarily leaves an open path from the hot cell interior to the operating area, and then replacing it with the new plug. All cables were preinstalled in the service plug and it was sealed before the evolution. The challenge was installing the heavy lead-shielded service plug without damaging the cables.

After installation in the hot cell, the load frame was cycled through several tests using surrogate materials to verify its operation.

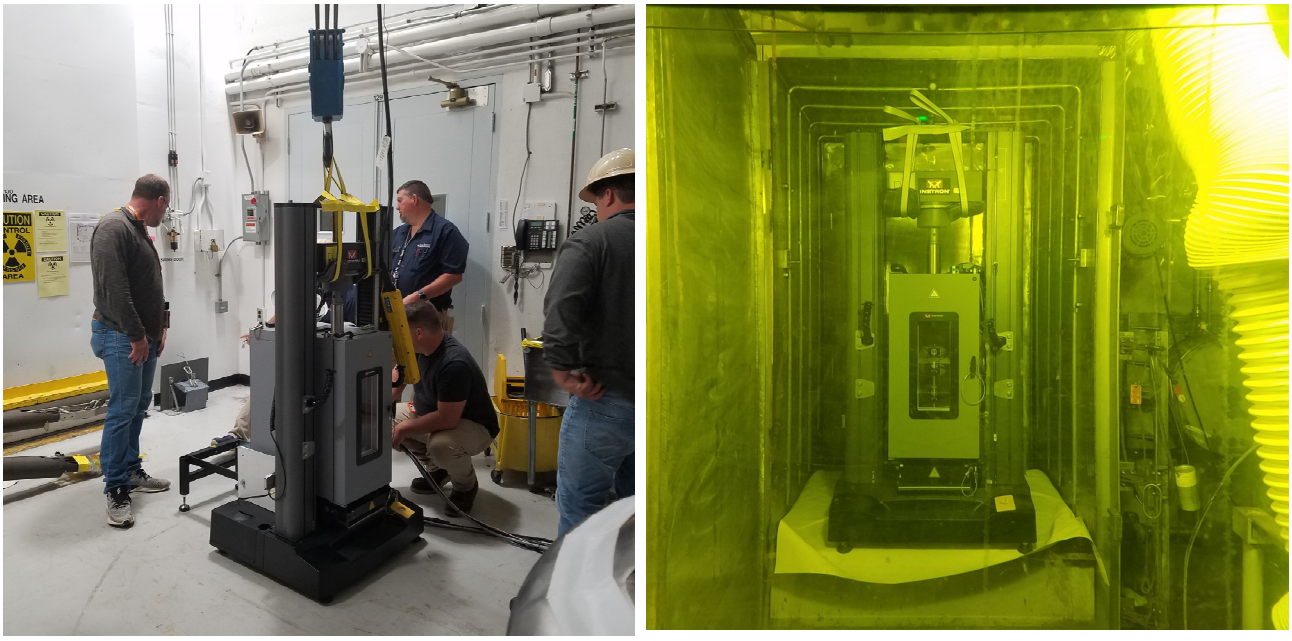

Figure E-1. The Instron load frame with its furnace was moved to the hot cell loading bay (left) and into the hot cell through the cell's primary airlock (right).

Figure E-2. The Instron load frame, with its furnace, was placed in the north hot cell (left) followed by the installation of the service plug containing all instrumentation and power (right).

E-2. Four-Point Bend Tests

The four-point bend (4PB) test provides values for the modulus of elasticity in bending (the *flexural modulus*) and the flexural stress and flexural strain response. It is traditionally the test used to study brittle materials in which the number and severity of flaws exposed to the maximum stress is directly related to the flexural strength and crack initiation. The load frame with its test fixturing (shown in Figure E-3) applies load at four points. The upper fixture is advanced at a selected fixed displacement rate in the downward direction, whereas the lower fixture is fixed and does not move. The fixture used is standard off-the-shelf equipment for 4PB, except that wire stops were added to ensure that the rod would not roll off the back of the fixture before the test could start. For tests at temperature, the load frame's furnace is pulled forward. The specimen is placed on the fixture, and the two are heated simultaneously to the test temperature. The stock furnace thermocouple was used to measure chamber temperature and a minimum 15 minutes of hold time at temperature was allotted to let the fixture and specimen reach steady state. ASTM C1161 – 18 [E-4] and ASTM D7264/D7264M – 15 [E-5] were used in setting up and evaluating the test data. ASTM E8/E8M – 16a [E-6] was used in evaluating the 0.2% offset yield strength.

Room temperature (RT) and 200°C tests were completed. The list of specimens is provided in Table E-1. Video and audio records of the tests were acquired along with the displacement and load. Each test segment was weighed before testing. A tray was placed below the specimen to catch debris, and the broken segments and debris were weighed following each test.

Several 4PB tests will be completed with the aerosol collection system to better quantify the size distribution and quantity of aerosol particles released during fracture. The aerosol tests have not yet been completed, as discussed in Appendix G.

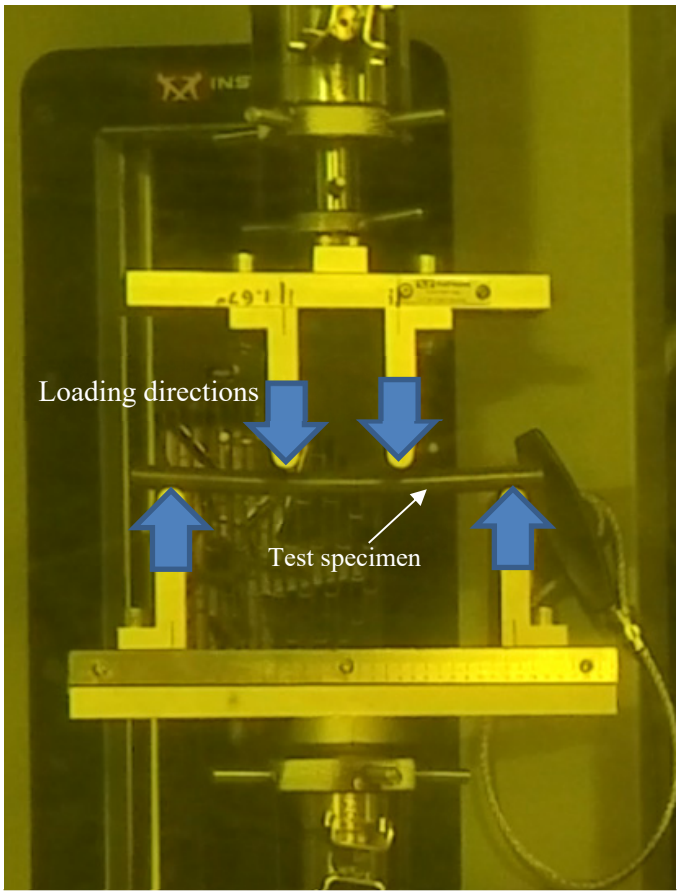

Figure E-3. The load frame configured for 4PB tests of a sister rod specimen.

Table E-1. List of specimens for 4PB.

Specimen ID			Cladding alloy	Test temp. (°C)	Specimen heat treatment before test	In-reactor operating zone	Specimen average burnup (GWd/MTU)	Specimen average oxide thickness (μ)	Test status
30AD05	850	1003	M5	200	None	zone1	60	3	Complete
30AD05	1003	1156	M5	RT	None	zone1	60	3	Future test with aerosol collection
30AD05	1299	1452	M5	RT	None	zone1	60	4	Complete
30AD05	1800	1953	M5	200	None	zone1	59	4	Complete
30AE14	825	978	M5	200	FHT*	zone1	58	4	Complete
30AE14	978	1131	M5	RT	FHT	zone1	59	4	Complete
30AE14	1800	1953	M5	RT	FHT	zone1	60	9	Future test with aerosol collection
30AE14	2050	2203	M5	200	FHT	zone1	60	10	Complete
3D8E14	872	1025	ZIRLO	200	None	zone1	64	10	Complete
3D8E14	1025	1178	ZIRLO	RT	None	zone1	64	11	Complete
3D8E14	1907	2060	ZIRLO	200	None	zone1	64	21	Complete
3D8E14	2810	2963	ZIRLO	RT	None	zone1	63	41	Future test with aerosol collection
3F9N05	872	1025	ZIRLO	200	FHT	zone1	59	10	Complete
3F9N05	1910	2063	ZIRLO	200	FHT	zone1	59	23	complete
3F9N05	2063	2216	ZIRLO	RT	FHT	zone1	59	28	Complete
3F9N05	2882	3035	ZIRLO	RT	FHT	zone1	58	46	Future test with aerosol collection
3A1F05	1279	1432	Zirc (LT)	RT	None	zone1	57	23	Complete
3A1F05	1432	1585	Zirc (LT)	200	None	zone1	56	34	Complete
3A1F05	2230	2383	Zirc (LT)	200	None	grid4	54	72	Complete
3A1F05	2402	2555	Zirc (LT)	RT	None	zone1	55	117	Future test with aerosol collection
F35P17	1319	1472	Zirc	RT	FHT	zone1	52	26	Complete
F35P17	1472	1625	Zirc	200	FHT	zone1	53	37	Complete
F35P17	2230	2383	Zirc	200	FHT	grid4	51	72	complete
F35P17	2402	2555	Zirc	RT	FHT	zone1	52	117	Future test with aerosol collection

* FHT = full-length fuel rod heat treatment

E-2.1 Test Procedure and Data Processing

E-2.1.1 Test Protocol

Instrument and software testing equipment description:

Load frame	Instron 5967
Bend fixture capacity:	30 kN
Voltage:	110/220 V
Software:	Bluehill-3
Furnace:	CP122117 Environmental Chamber and Control Unit
Furnace max temperature:	≤400°C
Scale:	Ohaus Scout NV1201

The 4PB fixture was adjusted before insertion into the hot cell with the lower support positions fixed at 5 in. center to center and the upper loading positions fixed at 1.67 in. center to center. The upper fixture is centered on the lower fixture, providing a symmetric loading of the rod specimen.

Each specimen is stored separately, and only one specimen is removed from its labeled storage container at a time. The specimen is weighed and then placed on the lower 4PB support fixture and pushed back until it rests against the provided stops. The upper 4PB fixture is lowered to within ~1/32 in. of the top of the test specimen.

If the test will be at temperature, the furnace door is closed and heating is initiated. During heating, the upper 4PB fixture is raised, as needed, to avoid preload of the specimen due to the thermal expansion of the system.

Once the system is at the specified temperature, the upper 4PB fixture is lowered to contact with the test specimen, as indicated by an increase in load. Care is taken to keep the amount of initial loading small.

The test system is then zeroed, and the test is initiated. All tests are run using a fixed displacement speed of 0.050 mm/s. The test proceeds until the specimen is fractured.

Following fracture, the specimen, as defined by the fueled pieces within the cladding, is weighed. Any loose particles are weighed. The posttest specimen is placed in a labeled capsule and returned to storage.

E-2.1.2 Test Specimen

Rough-cut 152 mm (6 in.) long fueled segments are used directly for 4PB. The specimens are unpressurized and have open ends.

E-2.1.3 Data Reduction

The 4PB test can be evaluated using simple beam theory and given the nominal dimensions of the rod specimen and test fixture.

The four-point loaded beam is preferred for determining strength properties because the center span is uniaxially stressed (i.e., no shear stresses exist). The bending moment applied is constant over the inner span between the two upper fixture loading points. The load applied on the specimen at each fixture loading point, P, is half the load recorded by the load frame. The deflection of the specimen at the loading points, Δ_f, is the measured crosshead translation of the upper test fixture recorded by the load frame.

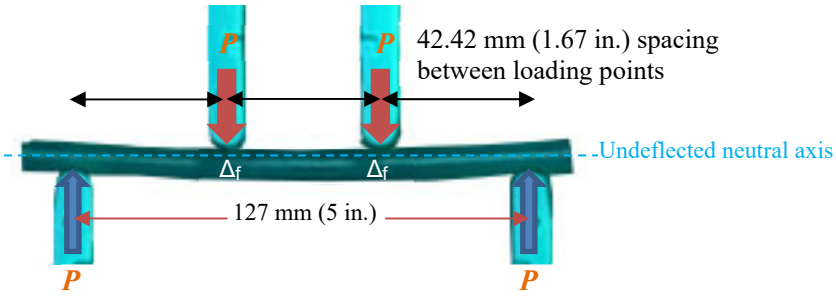

Figure E-4. Simple beam representation of the 4PB test.

To determine the maximum stress and strain on the specimen, the maximum bending moment between load upper loading points, M_{max}, is calculated as

$$42.42\ mm\ P. \tag{E-1}$$

Using classical beam theory, Δmax, the maximum beam deflection at the rod's axial center, can be calculated as:

$$\frac{Pa}{24EI}(3l^2 - 4a^2) = \frac{42.42\ mm\ P}{24EI}(3[127\ mm]^2 - 4[42.42\ mm]^2), \tag{E-2}$$

where E is the elastic modulus of the specimen, and I is the first moment of inertia, approximated as $\frac{1}{4}\pi\left(\frac{OD}{2}\right)^4 \approx 400\ mm^4$. Simplifying,

$$\Delta\,\text{max} = \frac{182.1\ mm^{-1} * P\ (in\ N)}{E\ (in\ N/mm^2)}. \tag{E-3}$$

Δ_f can also be related to the elastic modulus using beam theory:

$$\frac{Px}{6EI}(3la - 3a^2 - x^2) = \frac{42.42P}{6EI}(3 * 127\ mm * 42.42\ mm - 3[42.42\ mm]^2 - [42.42\ mm]^2),$$

which simplifies as:

$$\frac{158.5\ mm^{-1} * P\ (in\ N)}{E\ (in\ N/mm^2)}, \tag{E-4}$$

and allowing an estimate of the elastic modulus:

$$E = \frac{158.5\ mm^{-1} * P\ (in\ N)}{\Delta_f}. \quad \text{(E-5)}$$

Substituting Eq. (E-5) into Eq. (E-3) yields an estimate of the maximum deflection at the center of the 4PB specimen for use in calculating the maximum stress and strain:

$$\Delta\text{max} = (182.1 / 158.5)\ \Delta\text{f}\ . \quad \text{(E-6)}$$

The maximum stress, σmax, is estimated as:

$$\frac{42.42\ P\ (OD/2)}{I}\ . \quad \text{(E-7)}$$

For more accurate estimates, the measured outer diameter of the rod at the segment elevation [E-7] is used.

The maximum strain, εmax, is estimated as:

$$\frac{(182.1/158.5)\ \Delta f}{127\ mm}\ . \quad \text{(E-8)}$$

Ideally, the elastic modulus is equivalent to the flexural, or *bending*, modulus. Realistically, these values might be different. *E* is evaluated with the test data using Eq. (E-5).

Although the simplified beam approach is used to evaluate the test data, many of the assumptions used in this approach are not met, including the following.

- An SNF rod is not a homogeneous isotropic material.
- Transverse planes perpendicular to the longitudinal axis of the beam might not remain planar after the beam is deflected due to the many cracks and discontinuities inherent in the pellet stack.
- The maximum deflection measured was just over 12 mm, which is greater than the diameter of the rod tested and is not small compared with the beam depth.
- It is unclear whether any local plastic strain or twist occurred.

However, even in these circumstances, the results of the simple beam evaluations provide useful information.

Several ASTM standards are available for 4PB, including *Standard Test Method for Flexural Strength of Advanced Ceramics at Ambient Temperature*[E-4] and *Standard Test Methods for Flexural Properties of Polymer Matrix Composite Materials* [E-5], which were used to guide the selection of the fixture geometry and test gauge length.

E-2.2 Load and Displacement Data

The load vs. crosshead extension (i.e., displacement of the fixture) was recorded for each test and is provided in Figure E-5 for the baseline and heat-treated Zirc-4-clad and LT Zirc-4-clad specimens, in Figure E-6 for the baseline and heat-treated M5-clad specimens, and in Figure E-7 for the baseline and heat-treated ZIRLO-clad specimens. Figure E-8 plots the RT tests, and Figure E-9 plots the 200°C tests.

E-2.3 Corrections for Machine Compliance

The load vs. crosshead extension data necessarily includes the machine's compliance. When the load frame applies a force, the whole system, including the frame, load cell, grips, couplings, and specimen, experience some amount of deflection. The load frame reported displacement is the sum of entire system deformation. To determine the displacement of the specimen only, the machine compliance (deformation associated with the load frame, load cell, and grips) is removed from the load frame reported displacement data.

The machine compliance is measured by testing a rigid specimen using the 4PB setup. In this case, a high strength steel rod (OD=2.00") was used. The corrected displacement is calculated by subtracting the displacement reported in the machine compliance test from the displacement reported in the test of each sister rod specimen.

Because the 4PB specimens fracture at a low load in comparison with the load frame's limit (typically less than 10% of capacity), the correction made to the 4PB displacement is small.

E-2.4 Calculated Stress, Strain, 0.2% Offset Yield, Flexural Strength, and Flexural Rigidity

Using the simplified beam approach discussed in Section 2.1.3, stress and strain were calculated and are graphed in Figure E-10 at RT and Figure E-11 at 200°C. The flexural modulus, modulus of rigidity (EI), 0.2% offset yield strength, and flexural strength were also calculated. The supporting measured and calculated data are summarized in Table E-2 and plotted with specimen average burnup in Figure E-12 for RT tests and in Figure E-13 for 200°C tests.

The heat-treated M5 and ZIRLO-clad specimens generally have higher ductility than the baseline specimens, but it is difficult to come to any firm conclusions with the limited data available. Additional evaluations of the data will be completed in FY21.

Table E-2. Measured and calculated 4PB data.

Test specimen	Cladding alloy	Heat-treatment	Estimated Burnup (GWd/ MTU) [E-7]	Test temp. (°C)	Average Specimen OD [E-7]	Deflection at failure (mm)	0.2% Yield strength (MPa)	Flexural Strength (MPa)	Failure strain (%)	Flexural Modulus (MPa)	Flexural rigidity (N-m^2)
30AD05-1299-1452	M5	---	60	25.7	9.423	8.3	508	737	7.5	2.35E+04	9.1
30AE14-0978-1131	M5	FHT	59	26.6	9.459	11.7	473	700	10.6	2.27E+04	8.9
3D8E14-1025-1178	ZIRLO	---	64	25.3	9.500	7.4	570	880	6.7	2.39E+04	9.6
3F9N05-2063-2216	ZIRLO	FHT	59	24.7	9.471	10.6	509	823	9.6	2.20E+04	8.7
3A1F05-1279-1432	LT Zirc-4	---	57	26.4	9.465	5.8	580	830	5.2	2.39E+04	9.4
F35P17-1319-1472	Zirc-4	FHT	52	24.9	9.503	5.4	535	735	4.8	2.18E+04	8.7
F35P17-1472-1625	Zirc-4	FHT	53	27.2	9.531	6.5	533	795	5.9	2.25E+04	9.1
30AD05-0850-1003	M5	---	60	200.0	9.429	5.8	389	529	5.2	2.17E+04	8.4
30AD05-1800-1953	M5	---	59	200.0	9.423	6.1	420	577	5.5	2.31E+04	8.9
30AE14-0825-0978	M5	FHT	58	200.0	9.457	11.8	397	584	10.7	2.26E+04	8.9
30AE14-2050-2203	M5	FHT	60	200.0	9.454	12.3	380	584	11.1	2.16E+04	8.5
3D8E14-0872-1025	ZIRLO	---	64	200.0	9.497	7.1	471	748	6.4	2.23E+04	8.9
3D8E14-1907-2060	ZIRLO	---	64	200.0	9.492	7.2	464	730	6.5	2.17E+04	8.6
3F9N05-0872-1025	ZIRLO	FHT	59	200.0	9.465	7.9	440	669	7.1	2.11E+04	8.3
3F9N05-1910-2063	ZIRLO	FHT	59	200.0	9.469	9.1	424	676	8.3	2.10E+04	8.3
3A1F05-1432-1585	LT Zirc-4	---	56	200.0	9.459	5.2	485	681	4.7	2.21E+04	8.7
3A1F05-2230-2383	LT Zirc-4	---	54	200.0	9.480	5.1	464	644	4.6	2.07E+04	8.2
F35P17-2230-2383	Zirc-4	FHT	51	200.0	9.514	7.5	429	675	6.8	2.01E+04	8.1
					Average at RT:	8.0	530	786	7.2	2.29E+04	9.1
					Average at 200°C:	7.7	433	645	7.0	2.16E+04	8.5

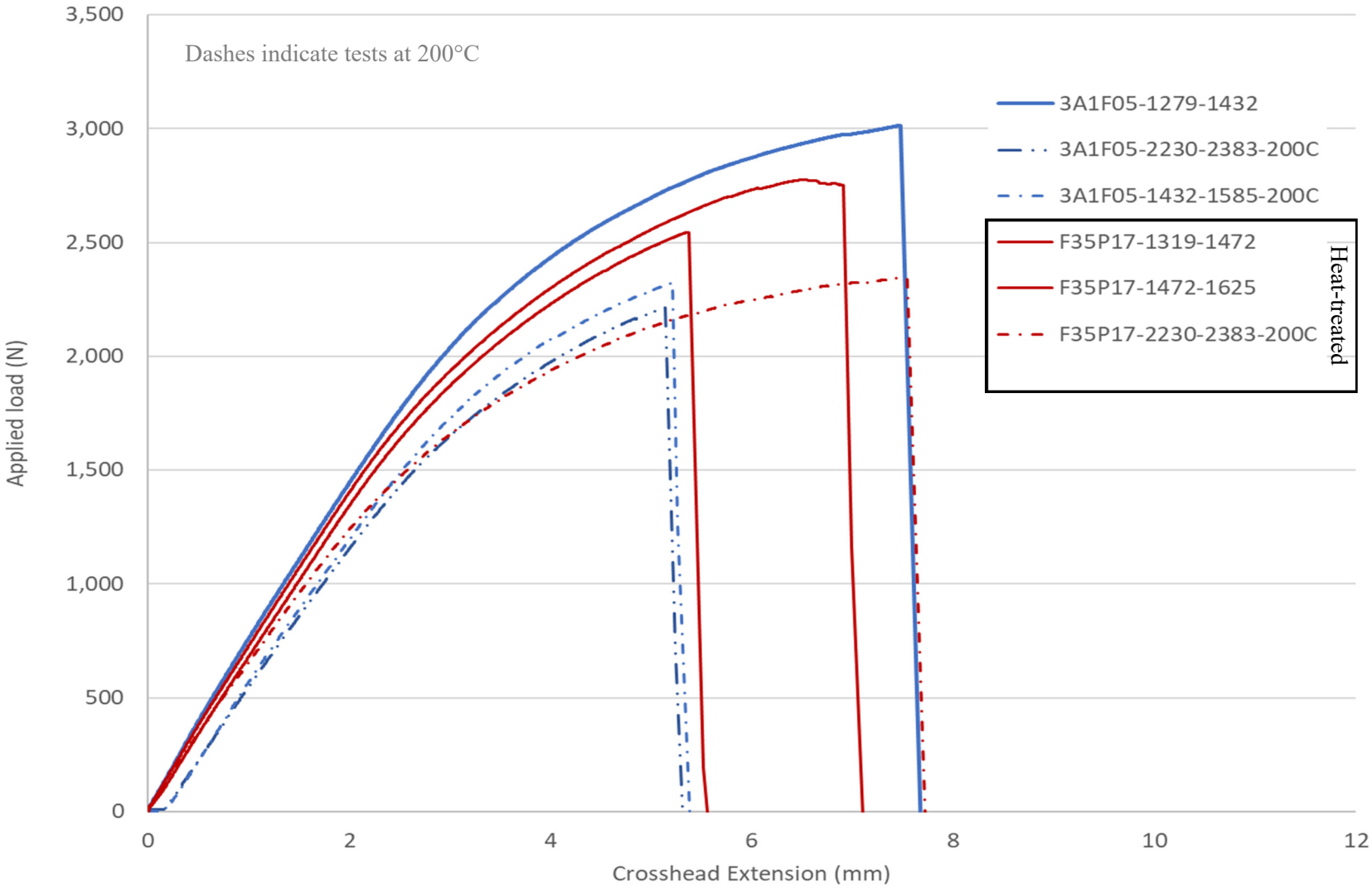

Figure E-5. Zirc-4 and LT Zirc-4 specimens, load vs. crosshead extension.

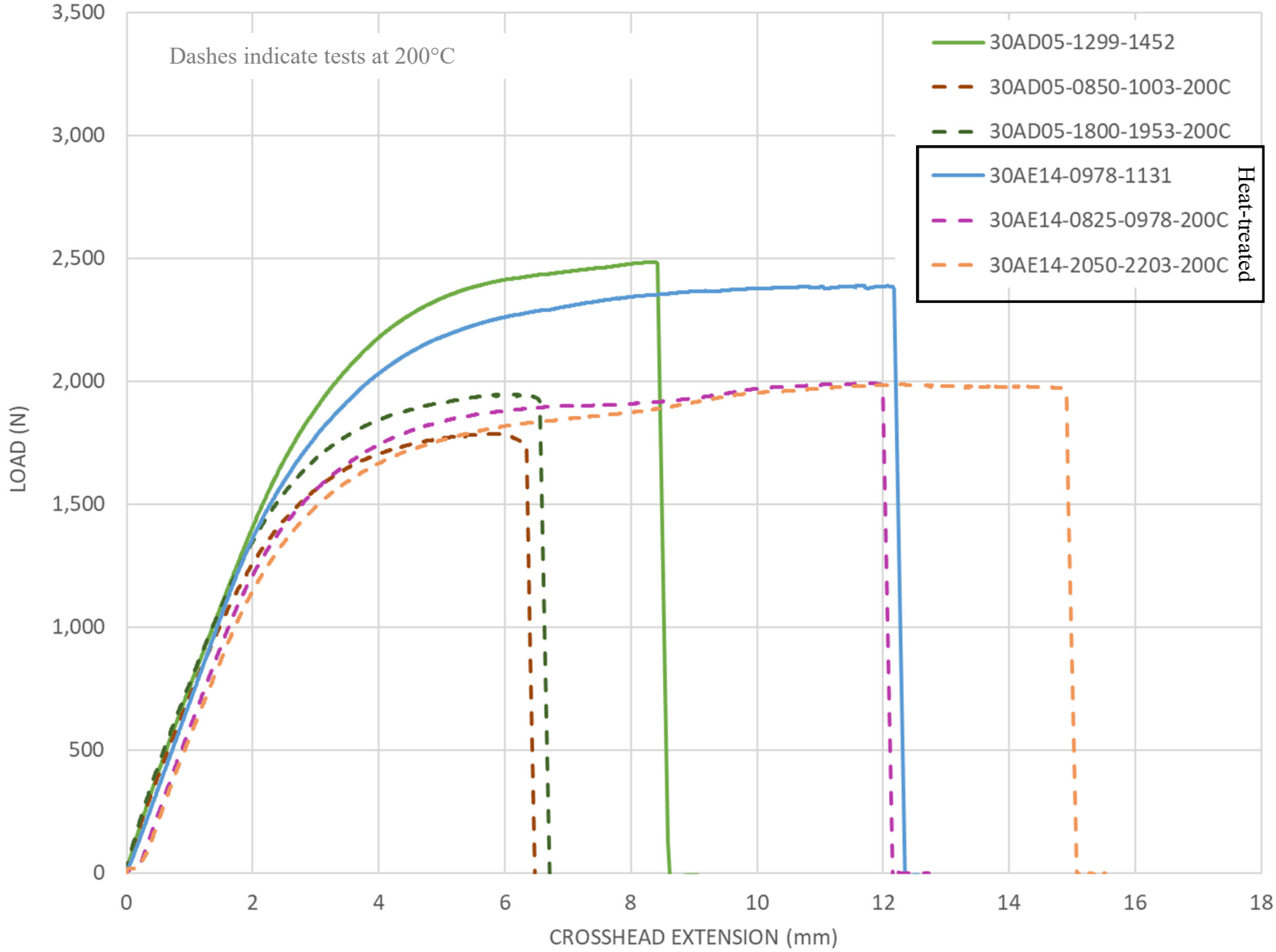

Figure E-6. M5 specimens, load vs. crosshead extension.

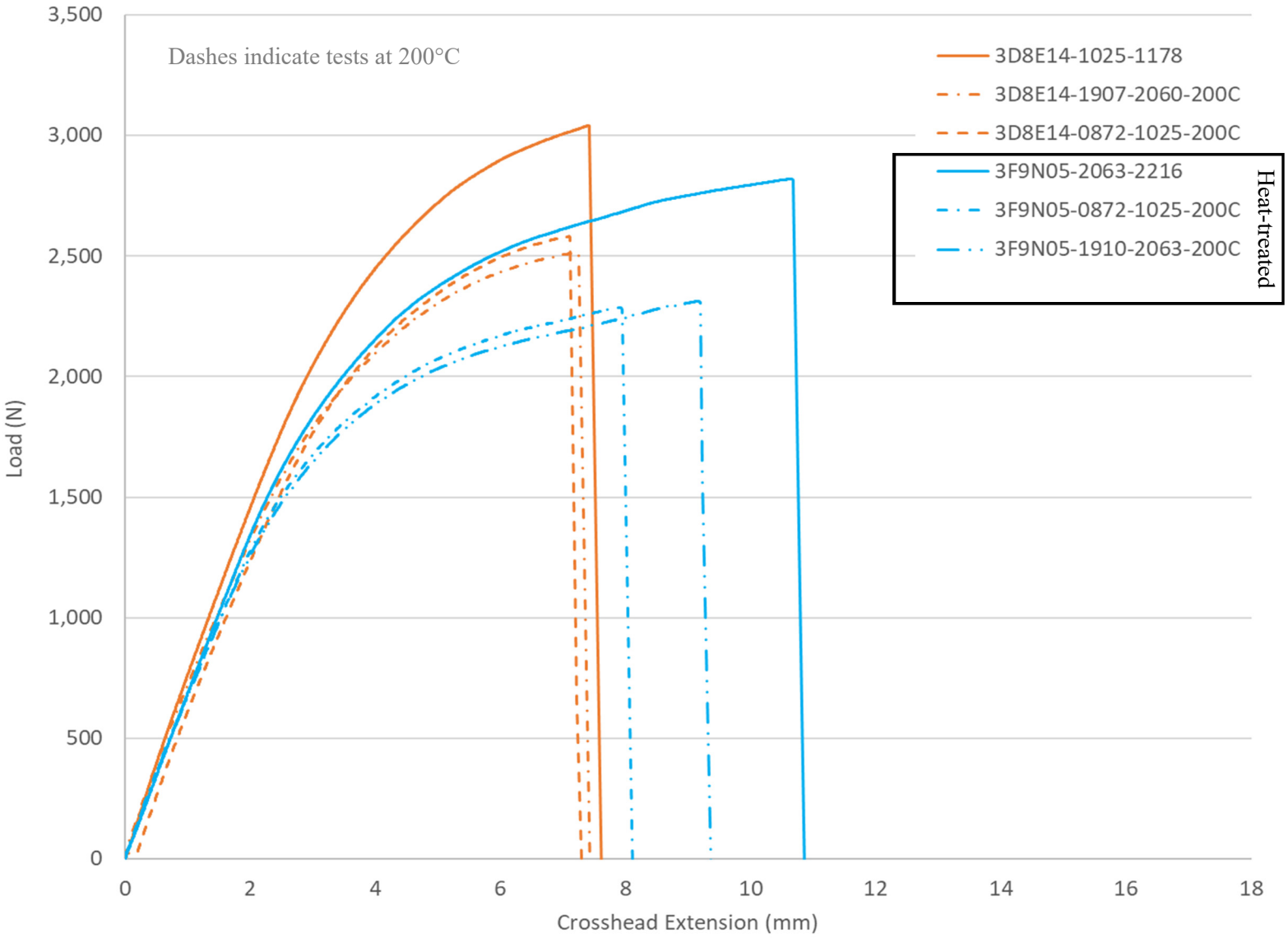

Figure E-7. ZIRLO specimens, load vs. crosshead extension.

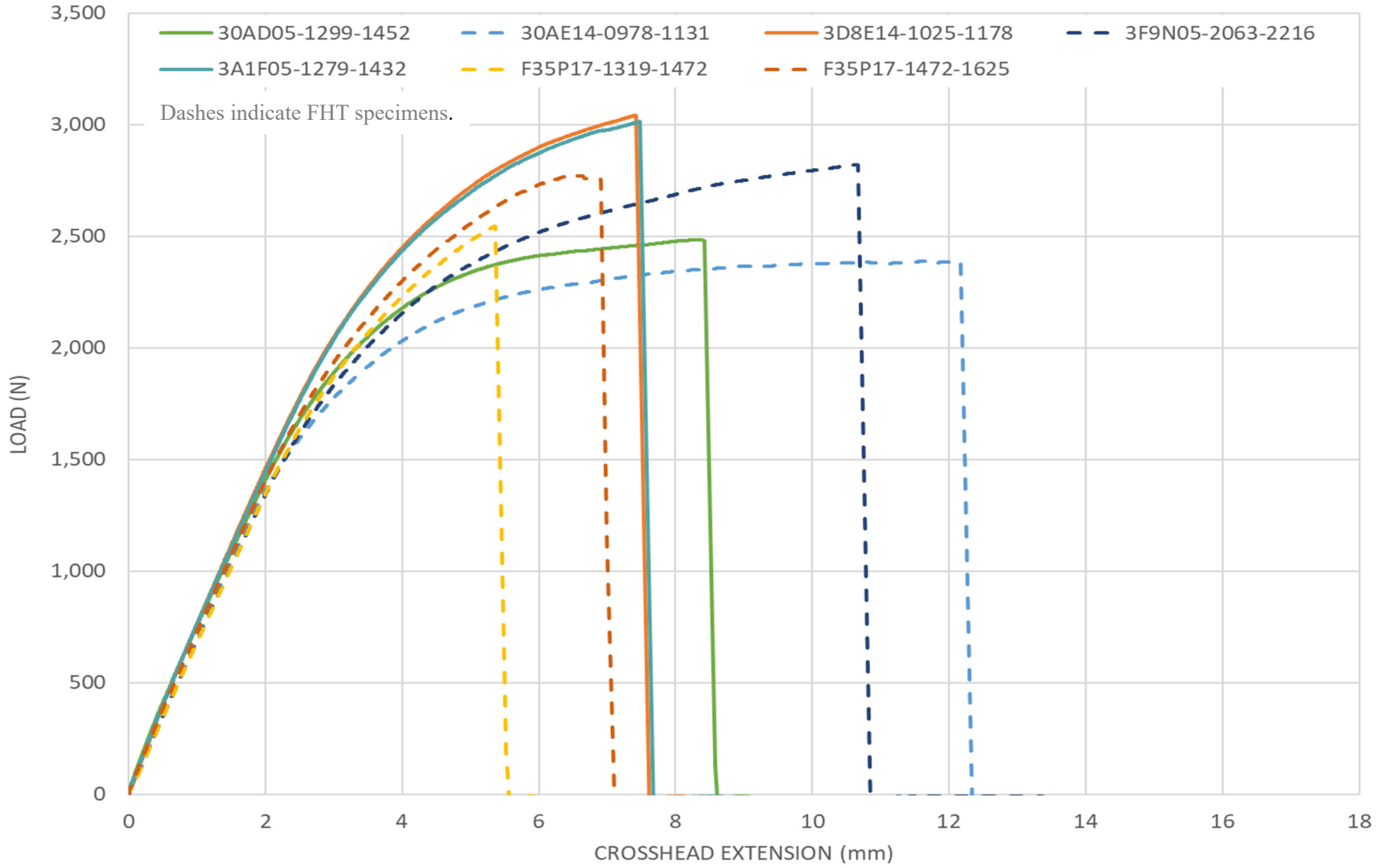

Figure E-8. Load vs. crosshead extension for all RT tests.

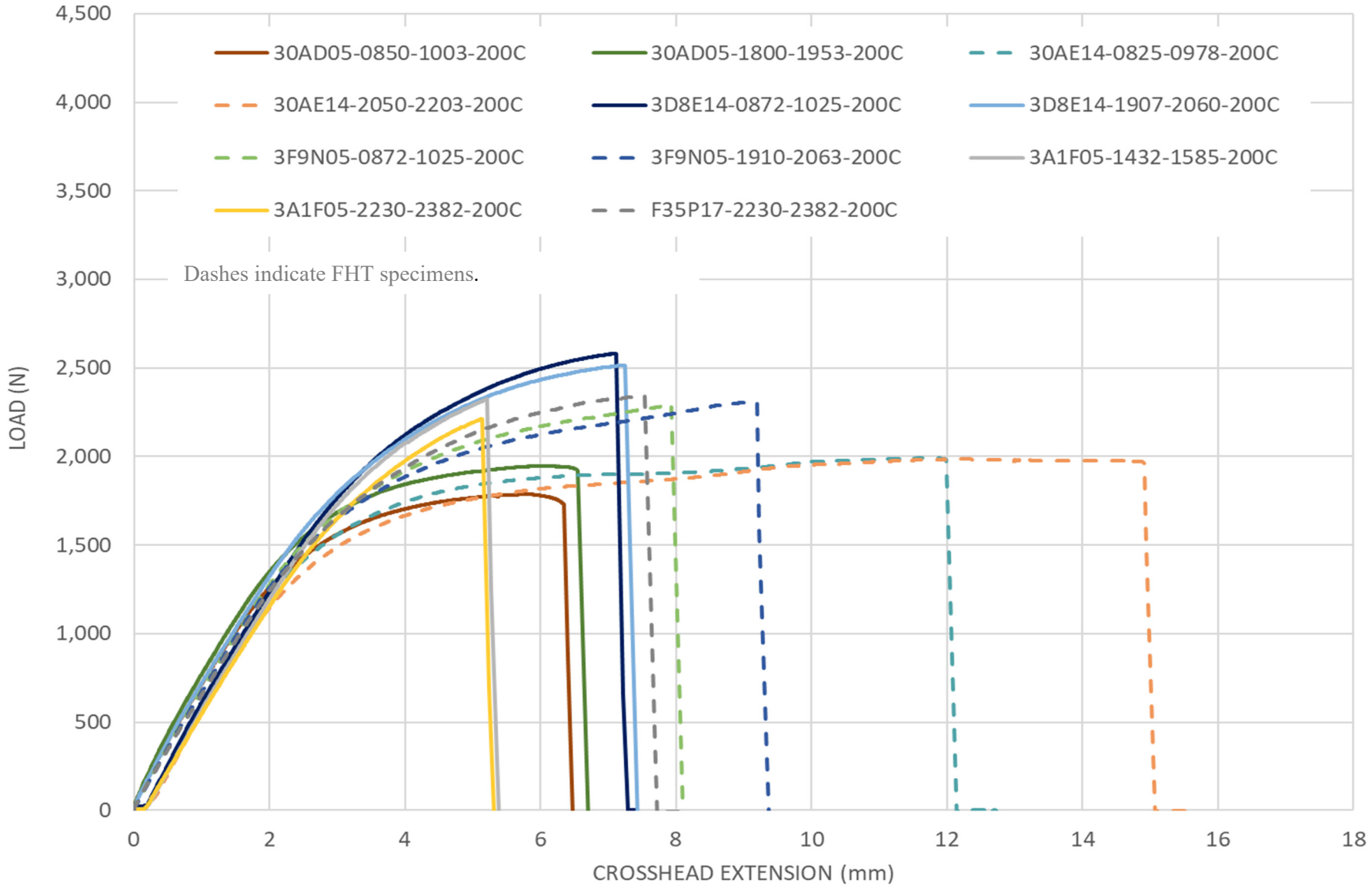

Figure E-9. Load vs. crosshead extension for all 200°C tests.

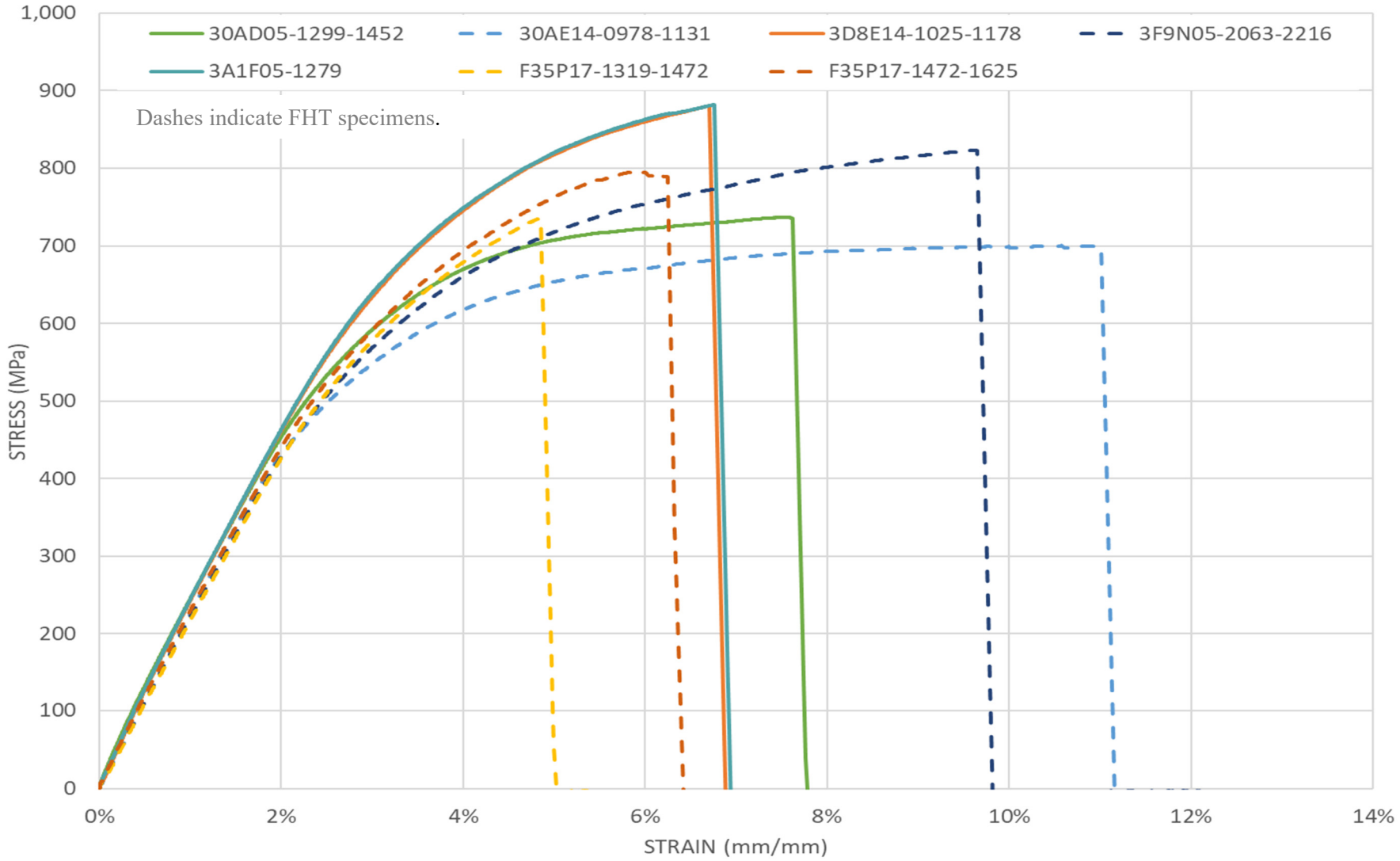

Figure E-10. Stress vs. strain plot for RT data.

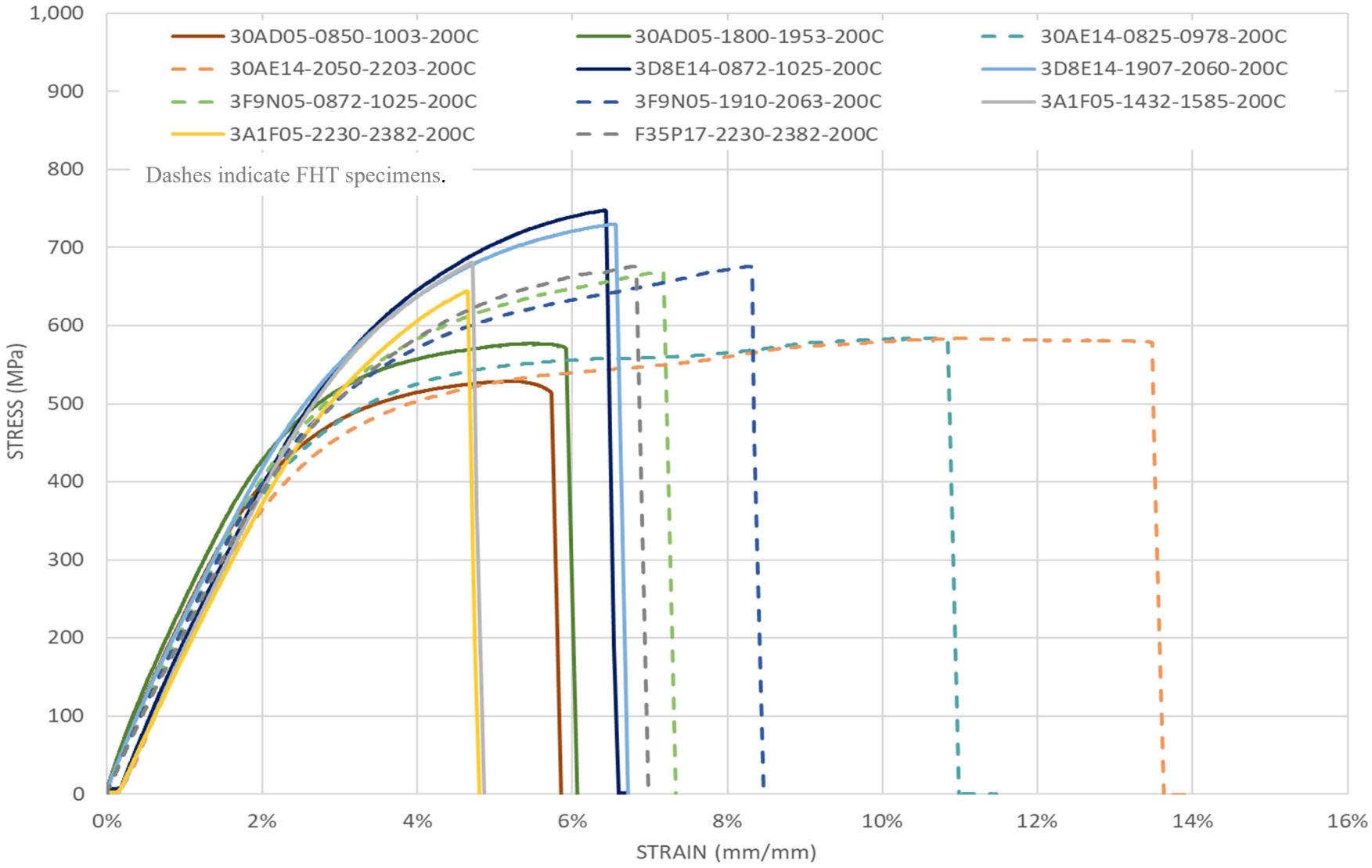

Figure E-11. Stress vs. strain plot for 200°C data.

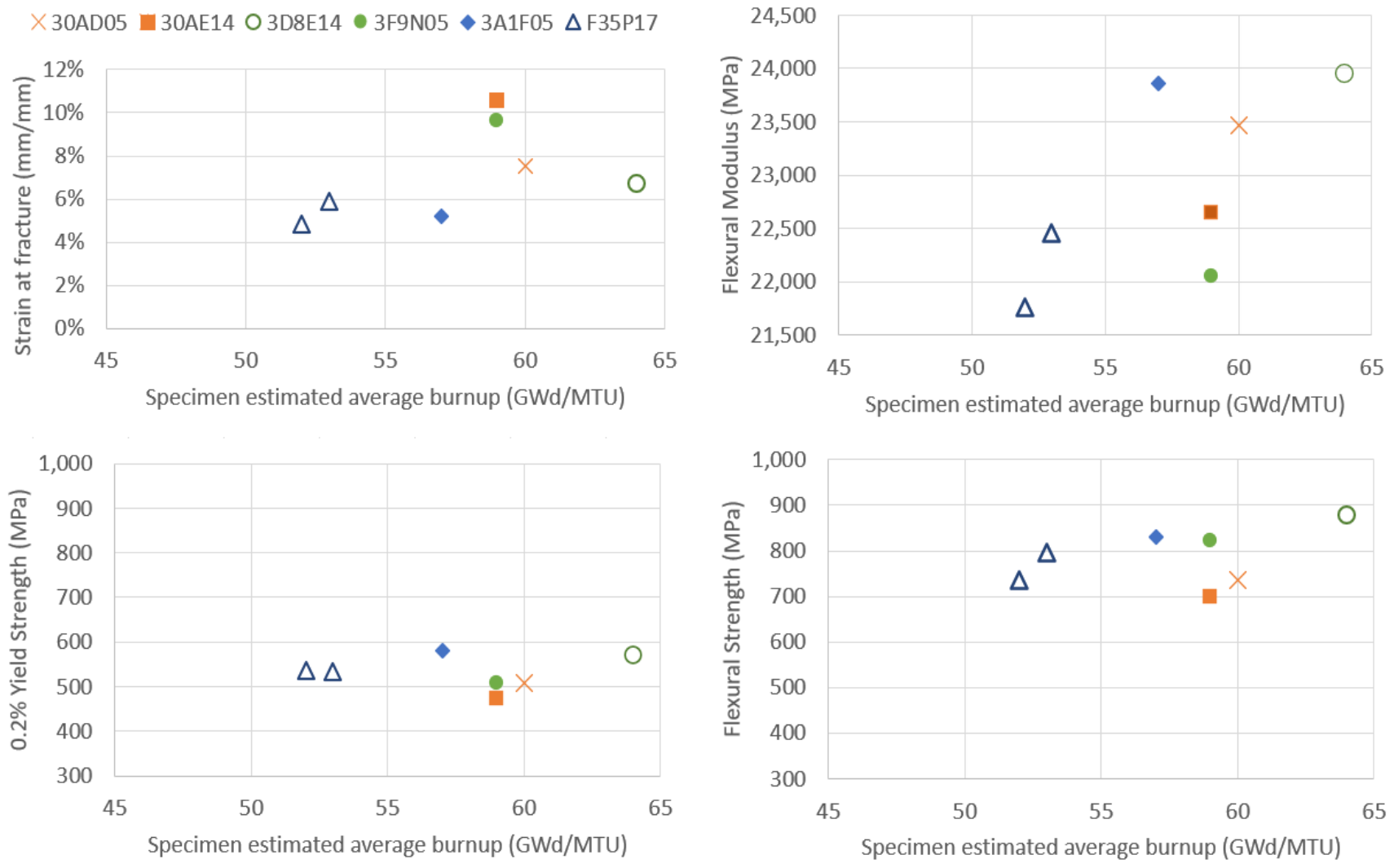

Figure E-12. Calculated RT data plotted as a function of specimen average burnup.

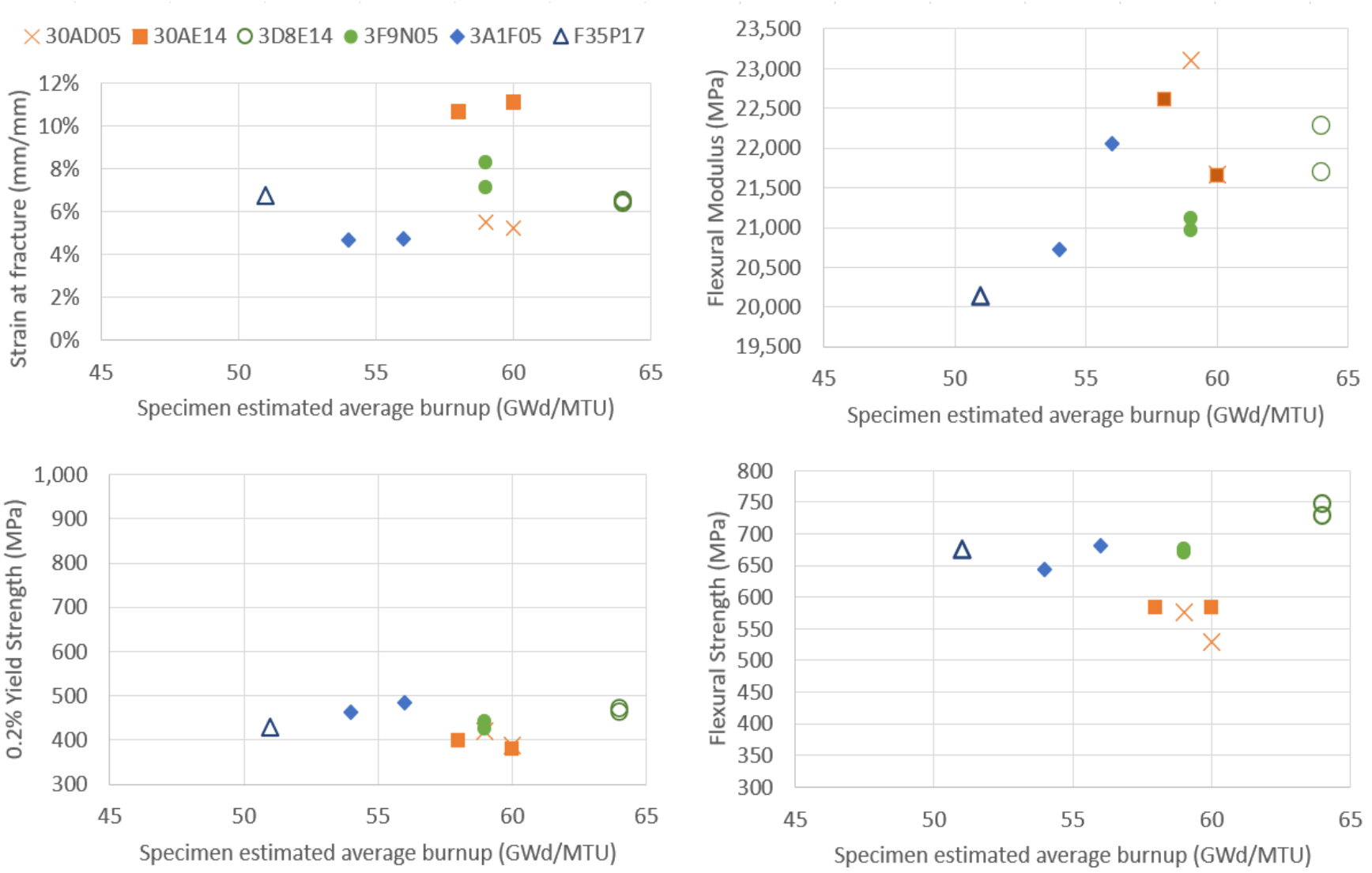

Figure E-13. Calculated 200°C data plotted as a function of specimen average burnup.

E-2.5 Typical Fracture Observed

All segments fractured near the center of the segment and in the gauge section. Many segments did not fracture completely through the rod section, as shown in Figure E-14(a). Although detailed imaging has not yet been completed, many segments appeared to fracture at pellet-pellet interfaces, as shown in Figure E-14(b). Other specimens fractured through the complete section with tearing of the cladding, as shown in Figure E-15(a) and Figure E-15(b), where the fracture also occurred in the body of the pellet.

Further imaging and evaluation of the fractures will be completed in FY21.

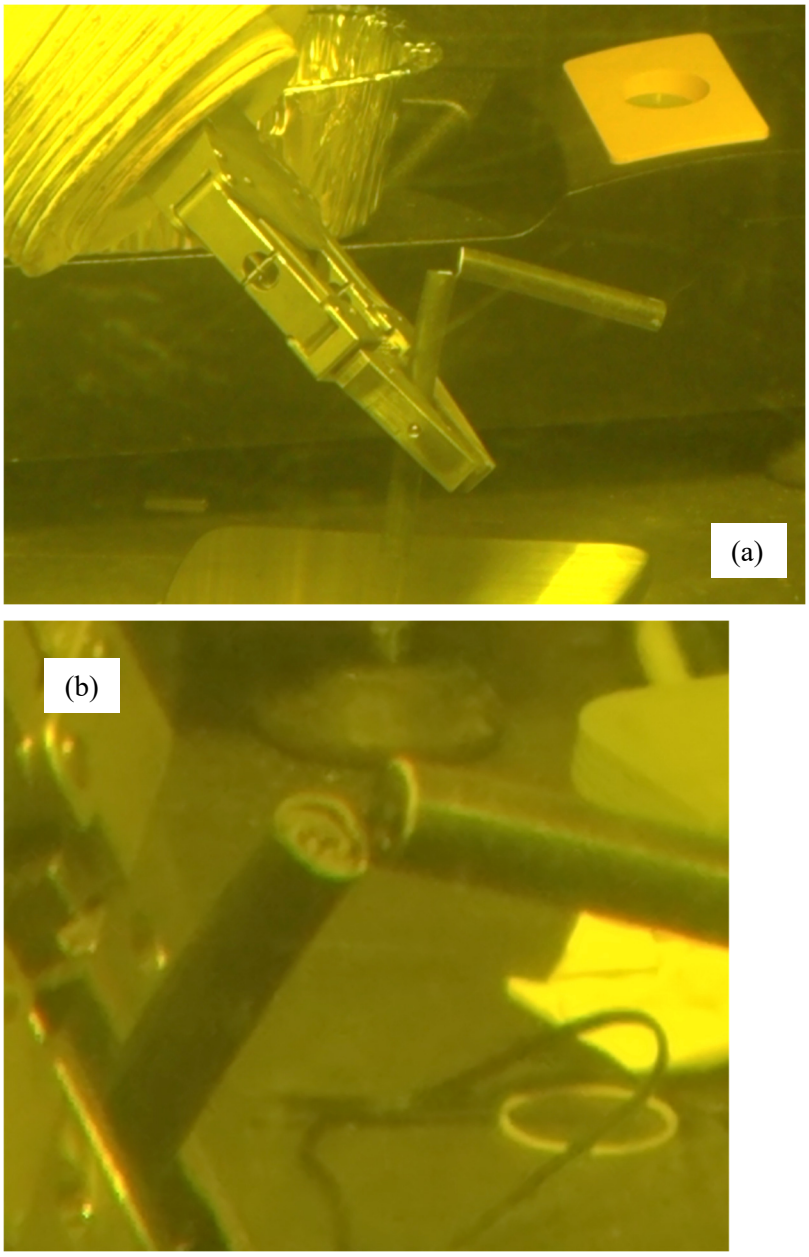

Figure E-14. (a) Many specimens did not completely fracture and (b) fractured at pellet-pellet interfaces.

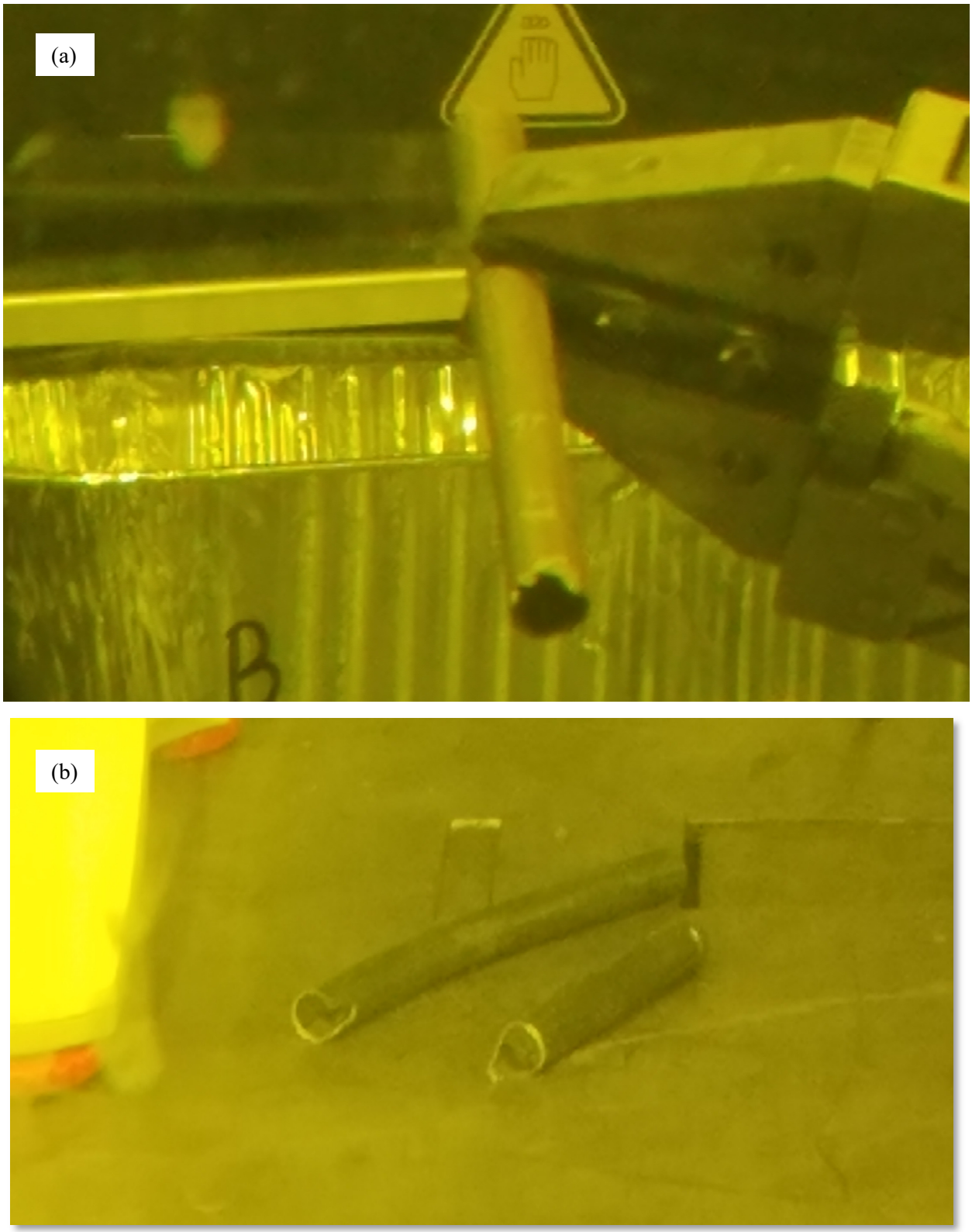

Figure E-15. (a) An example of through-section fracture with secondary tearing, and (b) fracture that occurred in the body of the pellet.

E-2.6 Fuel Release During Fracture

The amount of fuel released during fracture was monitored by weighing each specimen before and after the test and weighing the debris collected. Figure E-16 provides a histogram of the mass loss for all specimens tested in 4PB. The largest difference from pretest to posttest weight was 1.7 ± 0.1 g for F35P17-1472-1625 (RT test). Based on Figure E-17, there is not a trend of mass loss with test temperature or burnup. There is a tendency for the RT tests to have more mass loss, likely because the cladding fracture is more energetic than the 200°C fracture. From the nondestructive examinations [E-7], each pellet is 9.9–13.7 mm long on average[a] for the sister rods, with each pellet weighing approximately 5.1–7.0 g, assuming a density of 10.1 g/cc. Thus, the maximum mass lost represents about one-quarter of a pellet, whereas the more typical 0.4 g mass loss is less than one-tenth of a full pellet.

The catch tray placed below each specimen during testing collected most of the debris. As illustrated by Figure E-18(a) and (b), when fracture occurred at pellet-pellet ends, the debris consisted of small particles. If possible, the material on the catch trays will be imaged by scanning electron microscopy to determine the size of the particles.

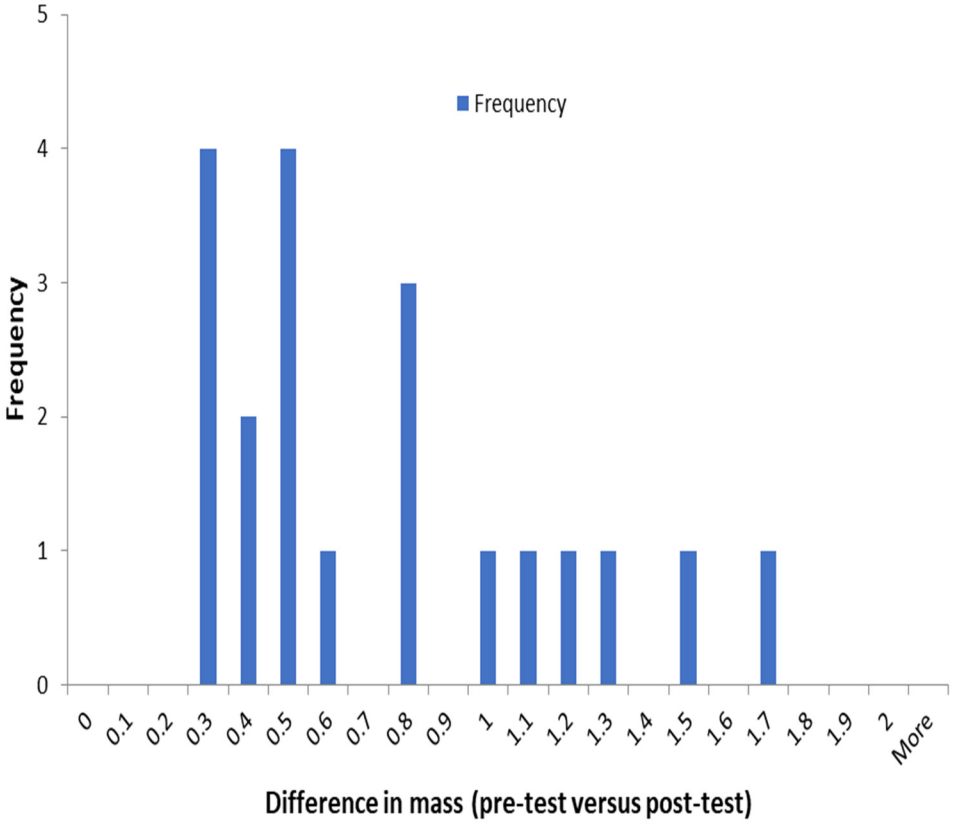

Figure E-16. Histogram of mass loss resulting in 4PB test.

[a]ZIRLO-, M5-, and LT Zirc-4-clad rods have measured pellet lengths from 9.8 to 10.3 mm, and the Zirc-4 clad rods have measured pellet length from 13.6 to 13.7 mm.

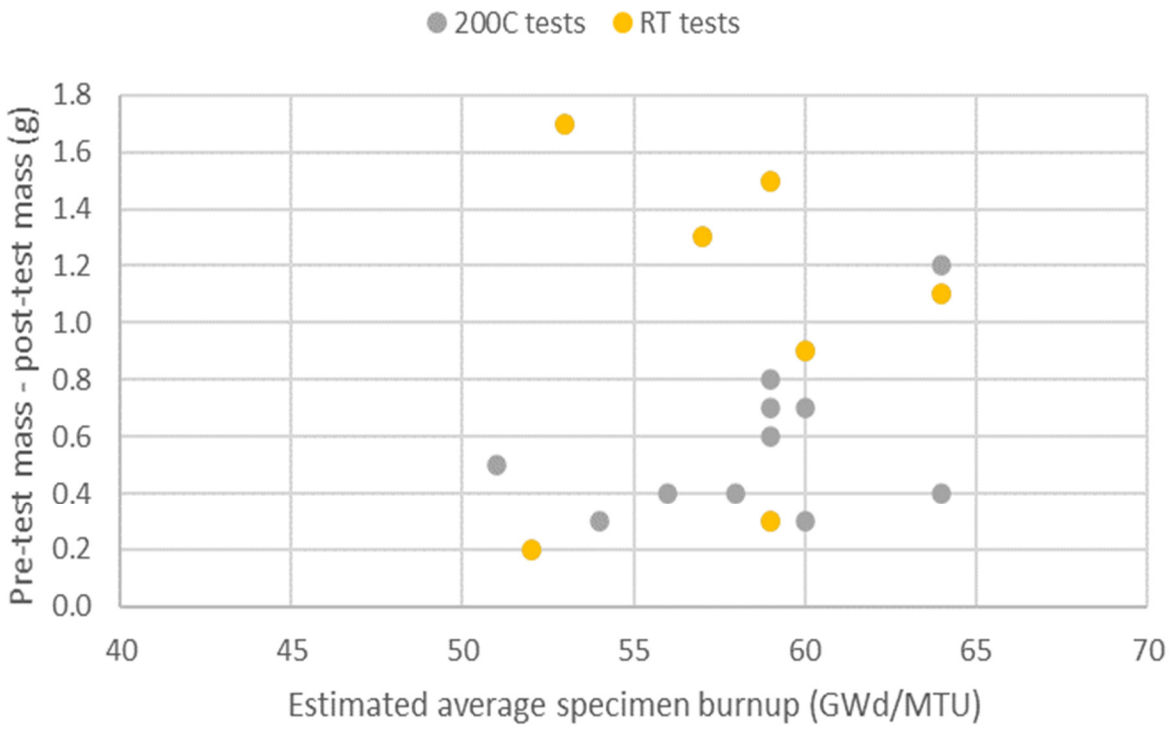

Figure E-17. Measured specimen mass differential (pretest and posttest) as a function of estimated average specimen burnup.

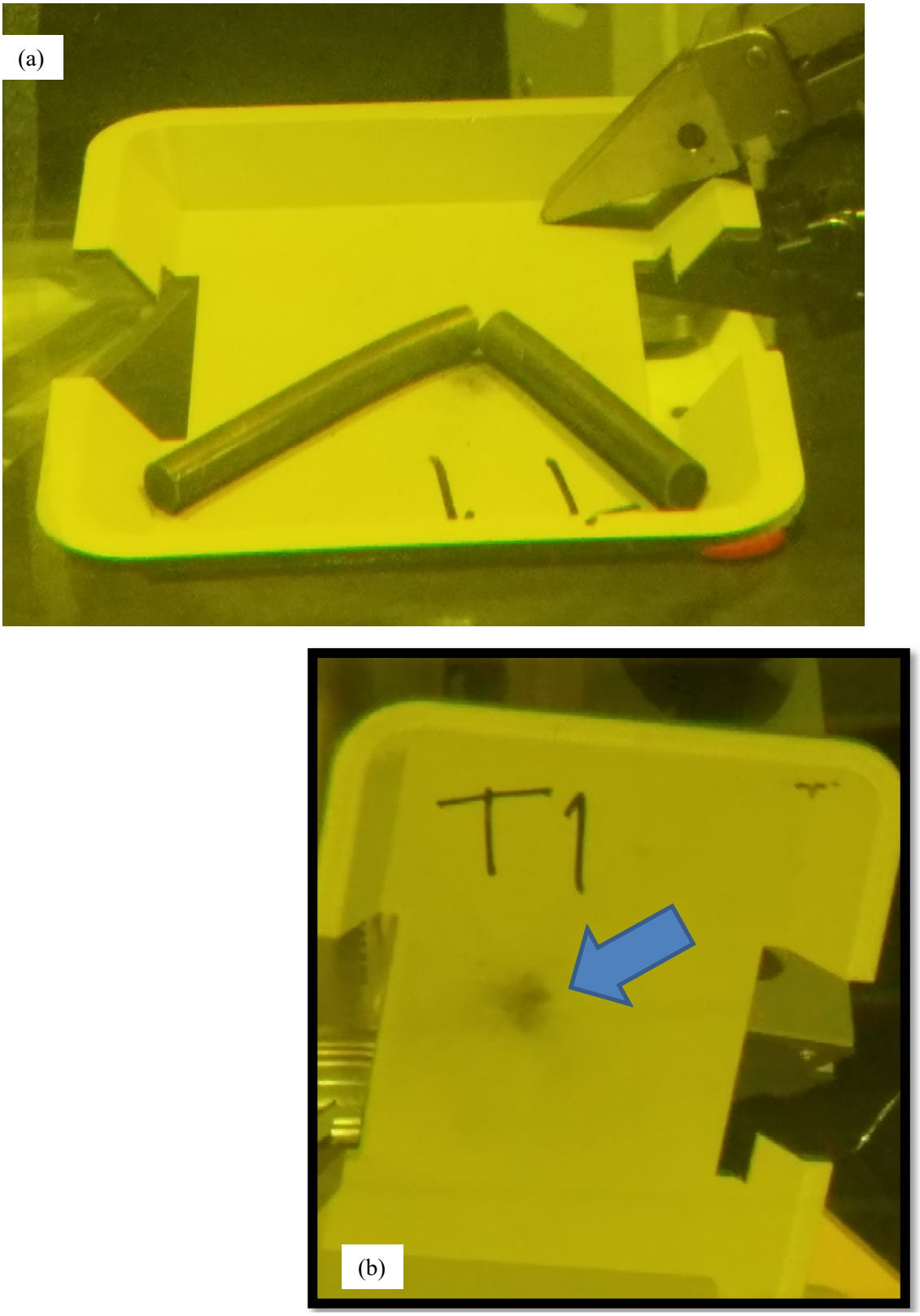

Figure E-18. (a) Posttest debris was captured by a catch tray located below the specimen with (b) the typical RT debris field composed of small particles.

E-3. Axial Tension Testing

To perform axial tension testing (DE.08), a small amount of fuel must be dissolved from each end of the specimen to allow for a grip to be inserted. The grip is used to prevent the specimen from being crushed at the load point. Therefore, although the rough-cut segments are available, they must be further processed to prepare them for the test. Table E-3 provides a list of the specimens to be tested.

Table E-3. List of specimens for axial tension testing.

Specimen ID			Test temperature	Specimen heat treatment before test	Operation zone	Specimen average burnup	Specimen average oxide thickness (μ)	Specimen alloy
30AE14	1574	1677	RT	FHT	zone1	59708	6	M5
30AD05	1452	1555	RT	None	zone1	59689	4	M5
30AE14	2300	2403	RT	FHT	zone1	59703	12	M5
30AD05	2802	2905	RT	None	zone1	56939	10	M5
F35P17	808	911	RT	FHT	zone1	53356	17	Zirc-4
3A1F05	1604	1707	RT	None	zone1	56669	42	LT Zirc-4
F35P17	2754	2857	RT	FHT	grid5	48531	133	Zirc-4
3A1F05	2754	2857	RT	None	grid5	52550	133	LT Zirc-4
3F9N05	1444	1547	RT	FHT	zone1	59480	12	ZIRLO
3D8E14	1553	1656	RT	None	zone1	64397	18	ZIRLO
3D8E14	2674	2777	RT	None	zone1	62923	44	ZIRLO
3F9N05	3138	3241	RT	FHT	zone1	55642	48	ZIRLO
30AE14	1471	1574	200°C	FHT	zone1	59199	5	M5
30AD05	1555	1658	200°C	None	zone1	59441	6	M5
30AE14	2403	2506	200°C	FHT	zone1	60227	13	M5
30AD05	3349	3452	200°C	None	zone1	49083	17	M5
F35P17	930	1033	200°C	FHT	zone1	53308	20	Zirc-4
3A1F05	1750	1853	200°C	None	zone1	56018	42	LT Zirc-4
F35P17	2857	2960	200°C	FHT	zone1	50566	138	Zirc-4
3A1F05	2857	2960	200°C	None	zone1	53978	138	LT Zirc-4
3D8E14	1450	1553	200°C	None	zone1	64219	16	ZIRLO
3F9N05	1547	1650	200°C	FHT	zone1	59371	13	ZIRLO
3D8E14	1804	1907	200°C	None	zone1	63962	19	ZIRLO
3F9N05	3035	3138	200°C	FHT	zone1	56996	48	ZIRLO

E-4. Microhardness Tests

The microhardness test (DE.09) equipment has been installed in the glove box. Specimens must be prepared for testing, which will commence once the priority metallographic mounts are completed because the microhardness preparation uses the same equipment and personnel. RT and 200°C tests are planned.

E-5. Ring Compression Tests

A significant body of data on cladding hydride reorientation and associated effects on cladding ductility was developed by Argonne National Laboratory (ANL) over the last decade with the most recent summary of results documented by Billone et. al. in 2019 [E-8]. Several baseline and heat-treated sister rod specimens were shipped to ANL for cladding ring compression tests (RCTs) and several specimens have been tested [E-8, E-9].

ORNL's data provide supplementary information on the load-bearing capability of intact fuel rods (cladding and pellets). Similar to the RCT of cladding specimens, the fueled rod segment is loaded across its diameter, and the load to specimen failure is measured.

E-5.1 Test Procedure and Data Processing

E-5.1.1 Test Protocol

Instrument and software testing equipment description:

Load frame	Instron 5967
Bend fixture capacity:	30 kN
Voltage:	110/220 V
Software:	Bluehill-3
Furnace:	CP122117 Environmental Chamber and Control Unit
Furnace max temperature:	≤400°C
Scale:	Ohaus Scout NV1201

The ring compression tests used a pair of 2 in. diameter flat steel compression platens rated to 30 kN. Each specimen is stored separately, and only one specimen is removed from its labeled storage container at a time.

The test specimen was centered on the lower platen using an elastomeric O-ring (RT tests) or a carriage washer (200°C tests). The upper platen was lowered to a position approximately 3 mm above the specimen.

If the test will be at temperature, then the furnace door is closed and heating is initiated. During heating, the upper RCT platen is raised, as needed, to avoid specimen preload due to thermal expansion of the system.

Once the system is at the specified temperature, the upper RCT platen is lowered to contact with the test specimen, as indicated by an increase in load. Care is taken to keep the amount of initial loading small.

The test system is then zeroed, and the test is initiated. All tests are run using a fixed displacement speed of 0.0125 mm/s. The test proceeds until the specimen is fractured.

Following fracture, the specimen, as defined by the fueled pieces within the cladding, is weighed. Any loose particles are weighed. The posttest specimen is placed in a labeled capsule and returned to storage.

E-5.1.2 Test Specimen

The RCT specimens were rough cut to 90 mm. The 90 mm specimens were sub-cut to ~25 mm long test specimens for RCT. Each specimen should contain two full pellets. The specimen was sized to avoid pellet loss from the unsupported ends that could invalidate the results and the 25 mm length was successful for that purpose.

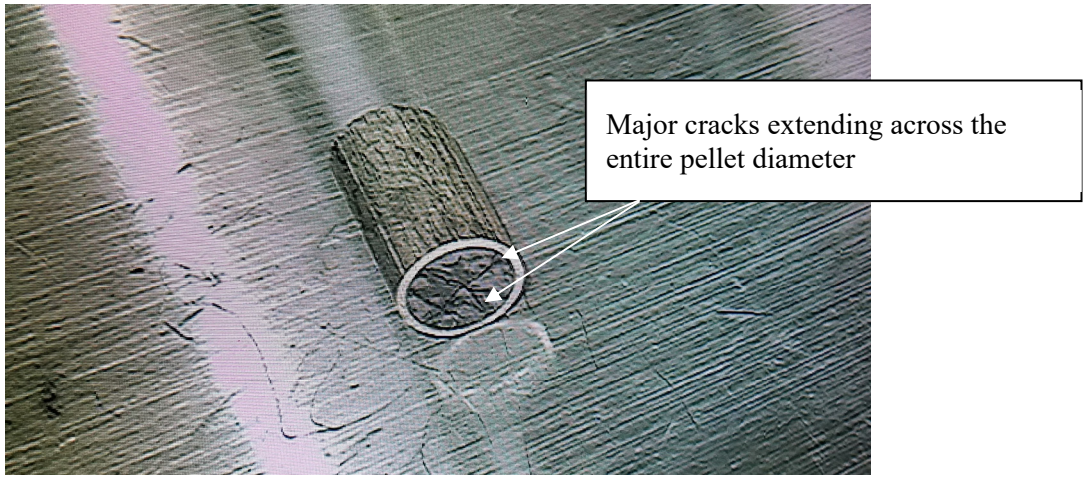

Figure E-19. Typical test specimen.

E-5.1.3 Data Reduction

A typical load vs. a displacement curve, as corrected for machine compliance, is shown in Figure E-20. The specimen takes on load, sometimes with a small drop as the operationally cracked pellets rearrange slightly, until the cladding fractures and the specimen splits open. If the test continues, then the section is crushed and eventually begins to take on load again as the pellet fragments are engaged in the load path. For purposes of this study, only the peak load achieved is reported.

As discussed in Section E-2.3, the load vs. crosshead extension data necessarily includes the machine's compliance. For RCT, the machine compliance is measured by testing an empty pressing die (more than ten times the load frame capacity) using the RCT setup. The corrected displacement is calculated by subtracting the displacement reported in the machine compliance test from the displacement reported in the test of each sister rod specimen.

As opposed to the 4PB specimens, the RCT specimens fracture at more than half of the load frame's limit and the correction made to the RCT displacement is significant. Figure E-21 plots the RCT compliance used in correcting the RCT specimen data.

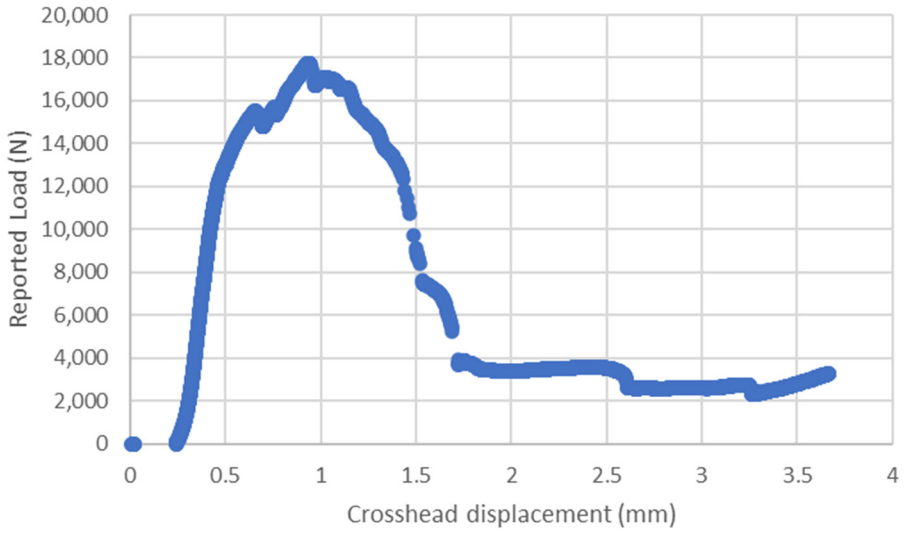

Figure E-20. Typical load vs. crosshead displacement for fueled RCT.

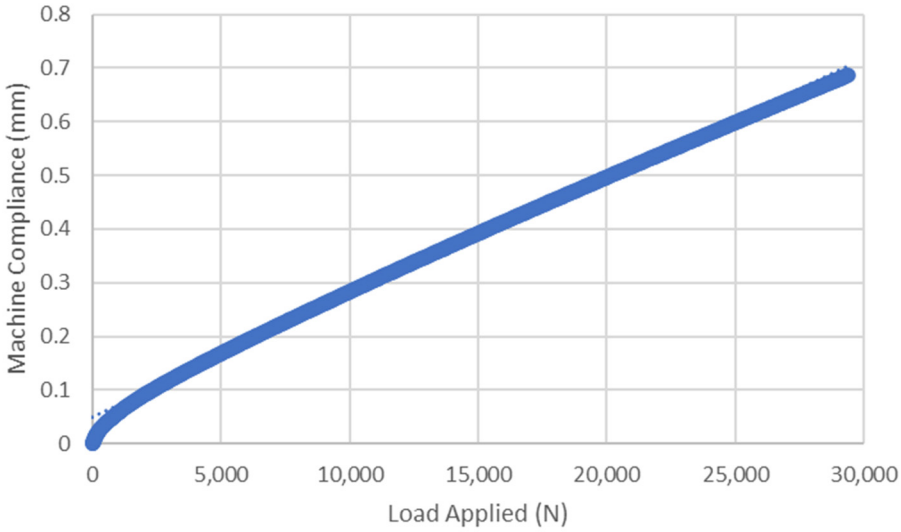

Figure E-21. Measured load frame compliance used to correct RCT data.

E-5.2 Peak Load Data

Table E-4 provides a listing of the peak loads recorded for the specimens tested in RCT. The average load-bearing capability of the segments in transverse compression is 16,415 N (3,690 lb_f). As shown in Figure E-22, there is not a trend with specimen average burnup, and there is not an appreciable difference in the maximum load from RT to 200°C. Cladding type also does not greatly influence the load-bearing capability and there is no difference related to the heat-treatment applied to some of the rods, as shown in Figure E-23.

Table E-4. RCT peak load data.

Sample ID	Test temperature (°C)	Cell temperature (°C)	Cladding alloy	Heat-treatment	Estimated specimen burnup (GWd/MTU)	Peak load (N)	Peak load (lb_f)
30AD05-2320-2345	25.2	25.2	M5	---	59	17,985	4,043
30AD05-3150-3175	25.3	25.3	M5	---	56	17,000[a]	3,822[a]
30AE14-2585-2610	25.9	25.9	M5	FHT	60	17,632	3,964
30AE14-3418-3443	25.9	25.9	M5	FHT	47	19,510	4,386
3D8E14-2322-2347	25.1	25.1	ZIRLO	---	64	15,788	3,549
3D8E14-3116-3141	25.1	25.1	ZIRLO	---	60	17,210	3,869
3D8E14-2347-2372	200	26.2	ZIRLO	---	64	17,752	3,991
3F9N05 -2482-2507	25.6	25.6	ZIRLO	FHT	59	17,444	3,921
3F9N05-3350-3375	25.6	25.6	ZIRLO	FHT	50	17,049	3,833
3F9N05-3375-3400	200	25.8	ZIRLO	FHT	50	18,683	4,200
3A1F05 -3124-3149	24.8	24.8	LT Zirc-4	---	52	12,303	2,766
3A1F05-2645-2670	24.9	24.9	LT Zirc-4	---	55	16,232	3,649
3A1F05-2670-2695	200	25.8	LT Zirc-4	---	55	12,384	2,784
F35P17-2645-2670	25.7	25.7	Zirc-4	FHT	51	12,476	2,805
F35P17-2960-2985	25.7	25.7	Zirc-4	FHT	50	12,961	2,914
F35P17-2670-2695[b]	200	25	Zirc-4	FHT	51	15,915	3,578
F35P17-2985-3010[c]	200	25.3	Zirc-4	FHT	50	12,500[a]	2,810[a]
					Maximum	20,732	4,661
					Minimum	12,303	2,766
					Average	16,415	3,690

a. The data file was not saved for this test. The value is from the estimate recorded in the laboratory notebook.
b. A major pellet crack as aligned with the loading direction.
c. A major pellet crack as aligned perpendicular to the loading direction.

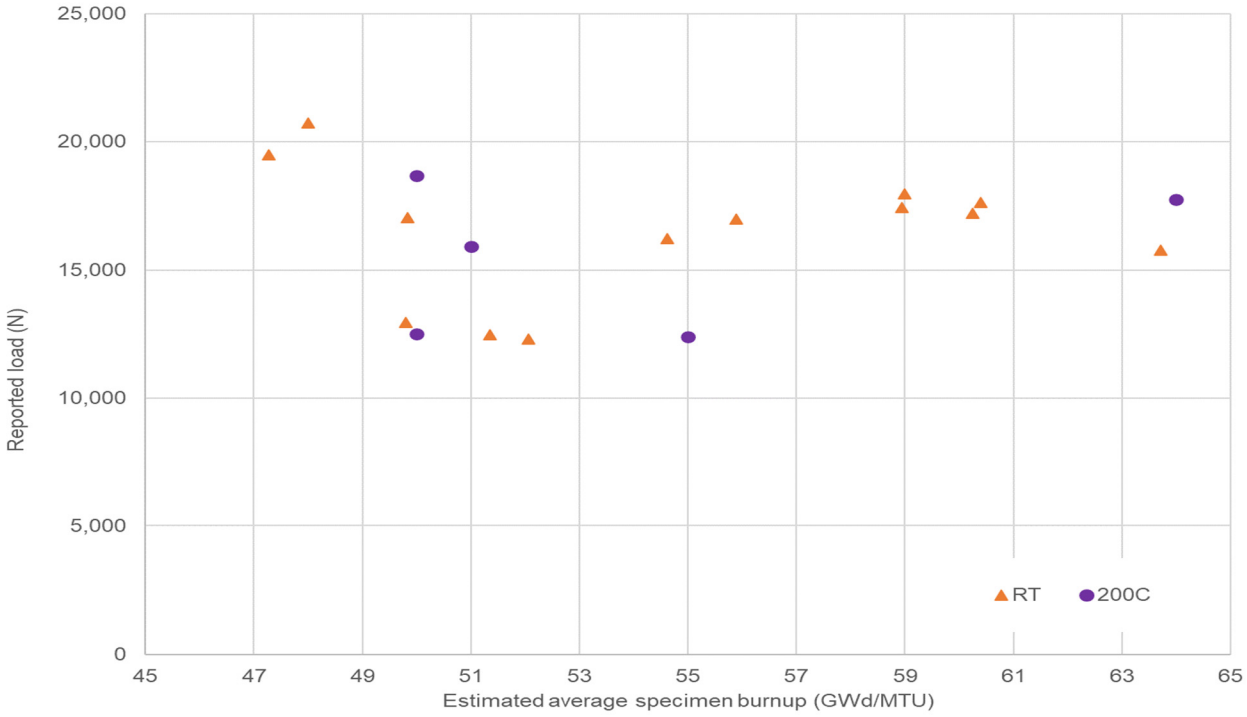

Figure E-22. Maximum RCT load vs. estimated average specimen burnup at RT and 200°C RCT.

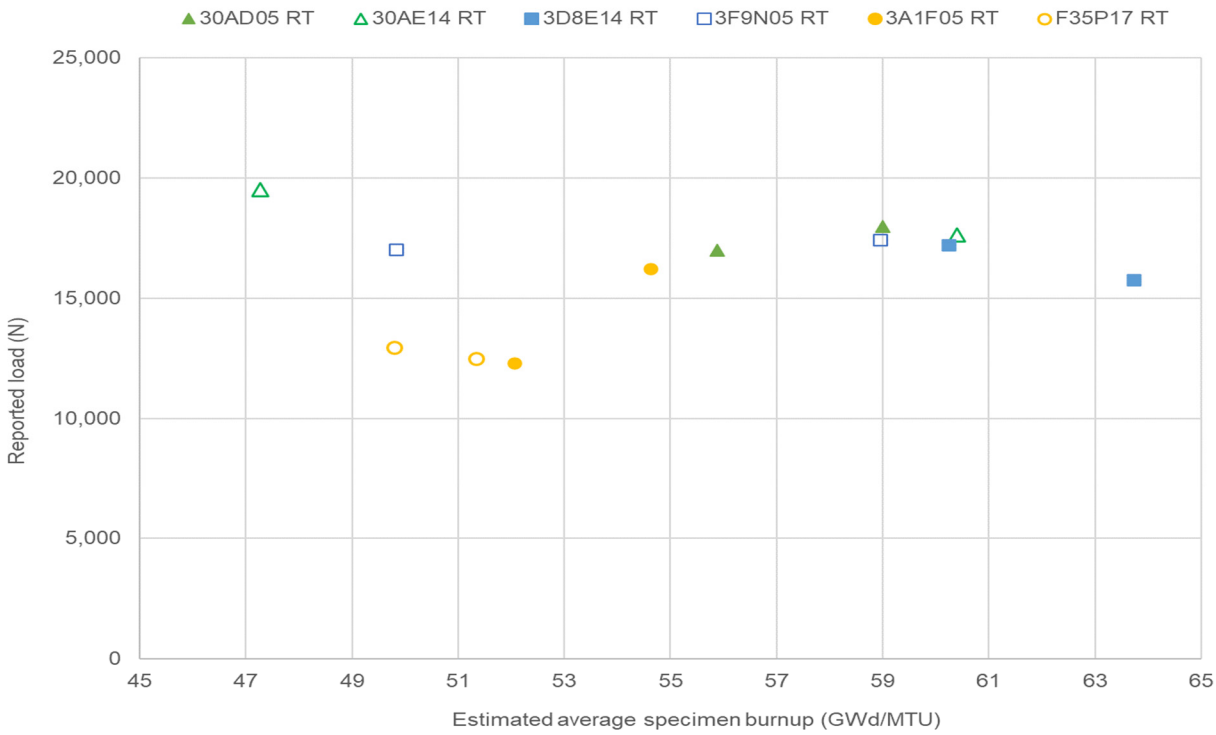

Figure E-23. Maximum RCT load vs. average specimen burnup at RT for baseline and FHT specimens.

A comparison of the results for a ZIRLO-clad fueled RCT is compared with a defueled ZIRLO RCT [E-9] in Figure E-24. The fueled cladding carries about eight times the load of the defueled cladding, but fractures at a much lower displacement because it is constrained by the pellet. The defueled RCTs predictably fracture at the 3 o'clock and 9 o'clock cladding positions [E-8,E-9], while the fueled RCTs fracture at a major pellet crack .

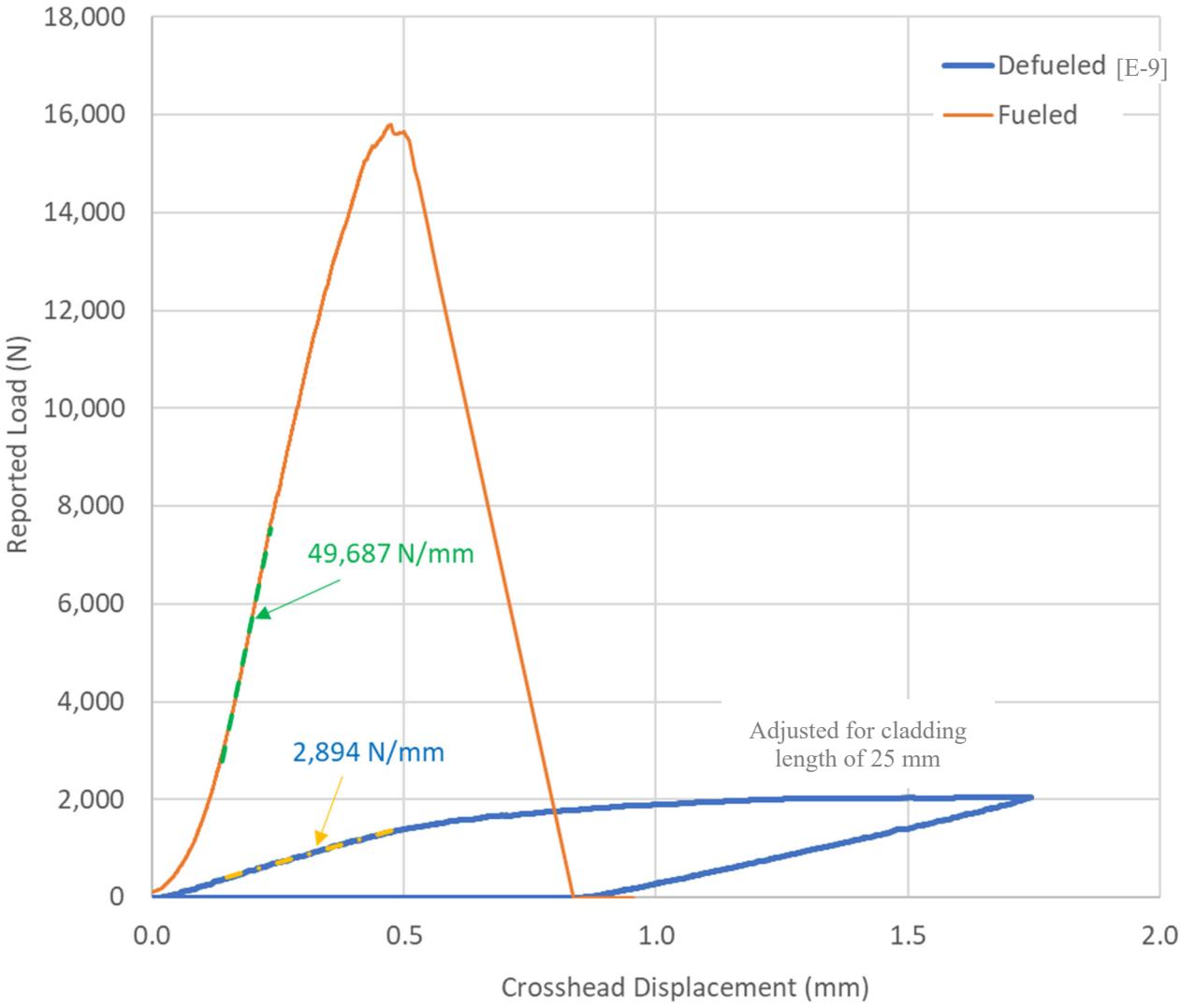

Figure E-24. Comparison of load vs. crosshead displacement for a ZIRLO Sister Rod specimen, fueled and defueled.

E-5.3 Typical Fracture Observed

The specimens typically carried load until at least one cladding fracture developed. As shown in Figure E-25, the specimen frequently broke into two equal halves. As the tests progressed, it became clear that fracture typically occurred at the location of one of the major diametrical pellet cracks, as illustrated in Figure E-26. Usually, there were two major cracks (defined as *full-diameter cracks*) visible at the end of the specimen. Two specimens from F35P17 were tested with the major crack aligned along the loading path and perpendicular to the loading path. There is a difference in the results for those two samples, but unfortunately the data were not recorded within the software for one of the tests, and only the notation on peak load in the laboratory notebook is available, which is not exact.

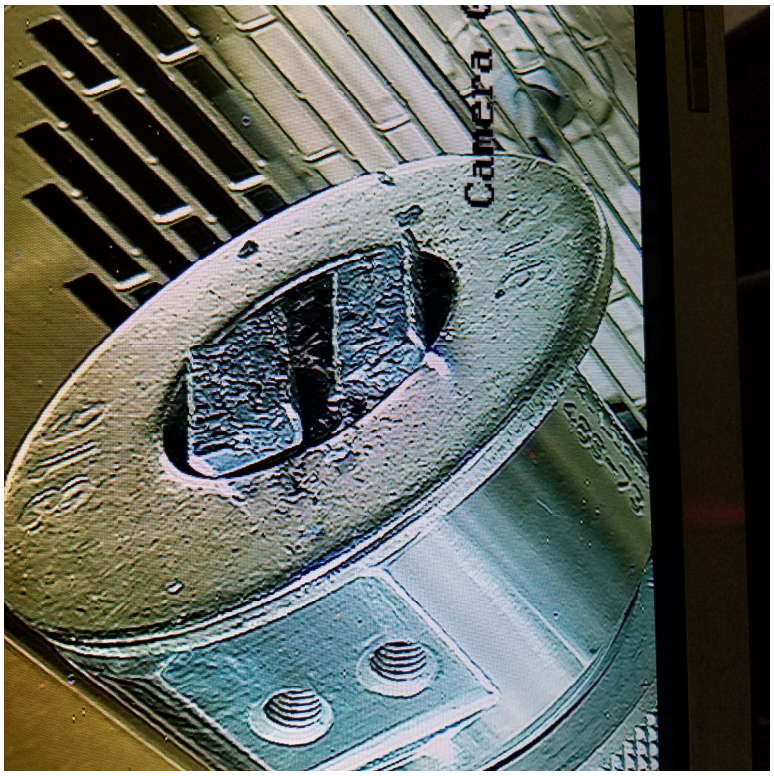

Figure E-25. Typical post-RCT appearance.

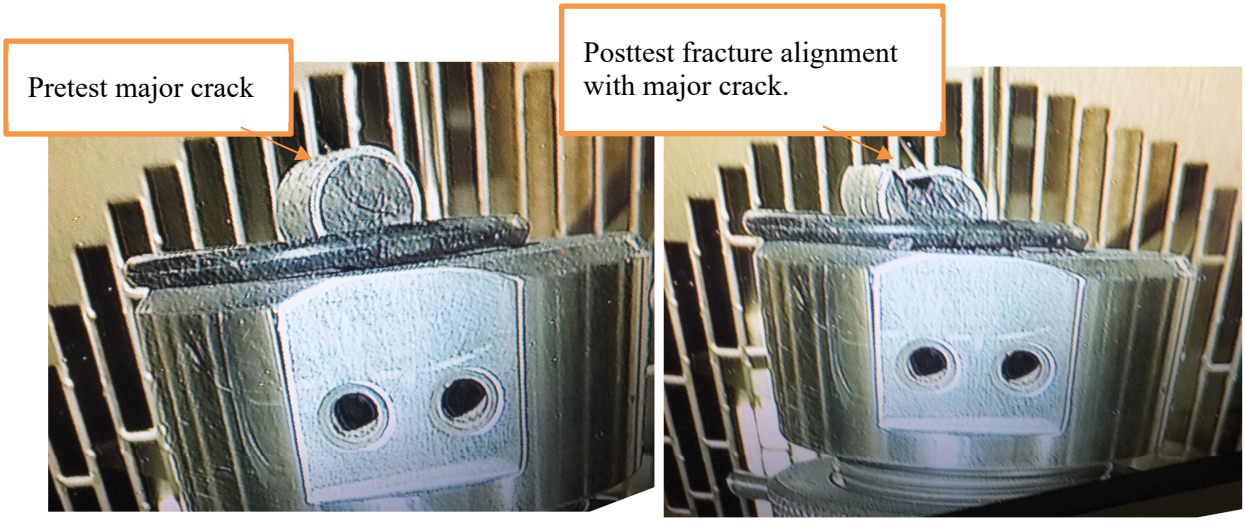

Figure E-26. RCT fracture path along major pellet crack.

E-6. Burst Tests

No progress has been made on configuring the available equipment for burst tests.

References

[E-1.] *High Burnup Dry Storage Cask Research and Development Project: Final Test Plan*, contract no. DE-NE-0000593, Electric Power Research Institute, Palo Alto, California (2014).

[E-2.] S. Saltzstein et al., *Visualization of the High Burnup Spent Fuel Rod Phase 1 Test Plan*, SAND2018-8042-O (2018).

[E-3.] R. A. Montgomery et al., *Post-Irradiation Examination Plan for High Burnup Demonstration Project Sister Rods*, SFWD-SFWST-2017-000090 ORNL/SR-2016/708, Oak Ridge National Laboratory, Oak Ridge, Tennessee, 2016.

[E-4.] ASTM International. (2018). ASTM C1161 – 18: Standard Test Methods for Flexural Strength of Advanced Ceramics at Ambient Temperature. West Conshohocken, PA: American Society for Testing and Materials.

[E-5.] ASTM International. (2015). ASTM D7264/D7264M – 15: Standard Test Methods for Flexural Properties of Polymer Matrix Composite Materials. West Conshohocken, PA: American Society for Testing and Materials.

[E-6.] ASTM International. (2016). ASTM E8/E8M – 16a: Standard Test Methods for Tension Testing of Metallic Materials. West Conshohocken, PA: American Society for Testing and Materials.

[E-7.] R. A. Montgomery et al., *Sister Rod Nondestructive Examination Final Report*, SFWD-SFWST-2017-000003 Rev. 1 (M2SF-17OR010201021) / ORNL/SPR-2017/484 Rev. 1 (ORNL/SPR-2018/801), Oak Ridge National Laboratory, Oak Ridge, Tennessee, 2019.

[E-8.] M. C. Billone, *Ductility of High-Burnup-Fuel ZIRLO™ following Drying and Storage*, ANL-19/14, M2SF-19AN010201011 Rev. 3, Argonne National Laboratory, June 30, 2019.

[E-9.] M.C. Billone, T.A. Burtseva, Y. Chen and Z. Han, Ductility of M5® and ZIRLO® Sibling Pin Cladding, M2SF-20AN010201012/ANL-20/47 (2020).